βQ114N and βT110V Mutations Reveal a Critically Important Role of the Substrate α-Carboxylate Site in the Reaction Specificity of Tryptophan Synthase[†]

Lars Blumenstein,[‡] Tatiana Domratcheva,[‡] Dimitri Niks,[§] Huu Ngo,[§] Ralf Seidel,[⊥] Michael F. Dunn,[§] and Ilme Schlichting*,[‡]

Max Planck Institute for Medical Research, Department of Biomolecular Mechanisms, Heidelberg, Germany, Department of Biochemistry, University of California at Riverside, Riverside, California 92521, and Max Planck Institute of Molecular Physiology, Department of Biophysical Chemistry, Dortmund, Germany

ABSTRACT: In the PLP-requiring $\alpha_2\beta_2$ tryptophan synthase complex, recognition of the substrate L-Ser at the β-site includes a loop structure (residues $\beta110−115$) extensively H-bonded to the substrate α-carboxylate. To investigate the relationship of this subsite to catalytic function and to the regulation of substrate channeling, two loop mutants were constructed: βThr110 → Val, and βGln114 → Asn. The βT110V mutation greatly impairs both catalytic activity in the β-reaction, and allosteric communication between the α- and β-sites. The crystal structure of the βT110V mutant shows that the modified L-Ser carboxylate subsite has altered protein interactions that impair β-site catalysis and the communication of allosteric signals between the α- and β-sites. Purified βQ114N consists of two species of mutant protein, one with a reddish color ($\lambda_{max} = 506$ nm). The reddish species is unable to react with L-Ser. The second βQ114N species displays significant catalytic activities; however, intermediates obtained on reaction with substrate L-Ser and substrate analogues exhibit perturbed UV/vis absorption spectra. Incubation with L-Ser results in the formation of an inactive species during the first 15 min with $\lambda_{max} \sim 320$ nm, followed by a slower conversion over 24 h to the species with $\lambda_{max} = 506$ nm. The 320 and 506 nm species originate from conversion of the α-aminoacrylate external aldimine to the internal aldimine and α-aminoacrylate, followed by the nucleophilic attack of α-aminoacrylate on C-4′ of the internal aldimine to give a covalent adduct with PLP. Subsequent treatment with sodium hydroxide releases a modified coenzyme consisting of a vinylglyoxylic acid moiety linked through C-4′ to the 4-position of the pyridine ring. We conclude that the shortening of the side chain accompanying the replacement of β114-Gln by Asn relaxes the steric constraints that prevent this reaction in the wild-type enzyme. This study reveals a new layer of structure−function interactions essential for reaction specificity in tryptophan synthase.

Pyridoxal phosphate-requiring enzymes play critically important roles in the metabolism of amino acids and some other amino-containing compounds (*10*, *11*). The classes of reactions catalyzed by PLP-dependent enzymes include decarboxylation, transamination, epimerization, β- and γ-eliminations, and β- and γ-substitutions. Tryptophan synthase is a PLP-requiring bienzyme complex that catalyzes the last two steps in the biosynthesis of L-Trp[1] (Scheme 1) (*10*, *12−14*). The α-site cleaves 3-indole-D-glycerol 3′-phosphate (IGP) to give indole and D-glyceraldehyde 3-phosphate (G3P) (Scheme 1A). The reaction sequence at the PLP-requiring β-site accomplishes the replacement of the hydroxyl group at C-β of L-Ser with the indolyl group derived from cleavage of IGP at the α-site. This reaction sequence occurs in two stages (Scheme 1B); in stage I, the external aldimine of L-Ser undergoes a β-elimination reaction to give the external aldimine of α-aminoacrylate, E(A-A); in stage II, indole,

channeled from the α-site to the β-site via a 25 Å tunnel, reacts with E(A-A) to give L-Trp. Hence the β-subunit is a member of the class of PLP enzymes that carry out β-replacement/β-elimination reactions, it belongs to the β-family (type II fold) of PLP enzymes (*15*), and the $\alpha_2\beta_2$ complex is an important paradigm for substrate channeling in a metabolic pathway (*4*, *7*).

[1] Abbreviations: $\alpha_2\beta_2$, native form of tryptophan synthase from *S. typhimurium*; α, the alpha subunit; β, the beta subunit; L, loops, and H, helices of the tryptophan synthase subunits; βQ114N, the β-site mutant enzyme with Gln114 replaced by Asn; βT110V, the β-site mutant enzyme with Thr110 replaced by Val; E(Ain), the internal aldimine intermediate; E(Aex₁), the external aldimine intermediate formed between the PLP cofactor and L-Ser; E(GD), the gem diamine species; E(A-A), the α-aminoacrylate external aldimine; E(Q₁), the L-Ser quinonoid intermediate; E(Q₃), the quinonoid intermediate that accumulates during the reaction between E(A-A) and indole; E(Aex₂), the L-Trp external aldimine intermediate; PLS, L-Ser pyridoxal phosphate external aldimine; PLP, pyridoxal phosphate; L-Ser, L-serine; L-Trp, L-tryptophan; IGP, 3-indole-D-glycerol 3′-phosphate; GP, α-D, L-glycerol phosphate; G3P, D-glyceraldehyde 3-phosphate; ASL, α-site ligand; F9, *N*-(4′-trifluoromethoxybenzenesulfonyl)-2-aminoethyl phosphate; TEA, triethanolamine; MVC, monovalent cation. Structural elements of tryptophan synthase are designated as follows: loop αL2, α53−α60; loop αL6, α179−α193; helix αH8, α249−α265; COMM domain, β102−β189; helix βH5, β145−β150; helix βH6, β165−β181; loop βL3, β109−β115 (*1*).

Scheme 1: Catalysis by Tryptophan Synthase[a]

[a] (A) The α-reaction consists of the cleavage of IGP to give indole and G3P. (B) The β-reaction occurs in two stages. In stage I, L-Ser reacts with enzyme-bound PLP to give the α-aminoacrylate external aldimine, E(A-A). In stage II, E(A-A) reacts with indole to give L-Trp and regenerates E(Ain), the internal aldimine form of the enzyme.

Scheme 2: Application of Dunathan's Hypothesis (*16, 17*) to Tryptophan Synthase[a]
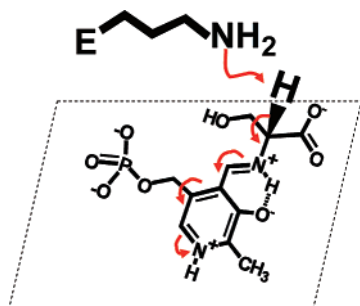
[a] According to the hypothesis, alignment of the C–H bond at C-α perpendicular to the plane of the PLP π-system of the external aldimine favors scission of this bond to give the resulting resonance-stabilized quinonoid intermediate.

The first step in virtually all reactions catalyzed by PLP enzymes involves substrate reaction with enzyme-bound PLP to give an external aldimine species, for example E(Aex₁) in Scheme 1B (*11*). Dunathan's hypothesis (*16, 17*) provides a mechanistic framework for understanding the diversity of reactions arising from this common intermediate. Dunathan proposed that reaction specificity arises from alignment of the scissile bond perpendicular to the plane of the PLP π-system so that the anion derived from bond cleavage becomes delocalized, both in the transition state and in the resulting resonance delocalized carbanion, the quinonoid intermediate (as shown in Scheme 2).

Substrate specificity has long been a subject of interest for the PLP-requiring enzymes especially in the α-family (type I fold). For example, interactions at the substrate binding sites of the aspartate amino transaminases (AspATs) are dominated by charge–charge Coulombic interactions involving an Arg residue in the side chain subsite and an Arg residue in the α-carboxylate subsite. These arginine residues (R292 and R386, respectively, in *E. coli* AspAT) function to lock the substrate into the correct position for reaction and are derived from different subunits. Cronin and Kirsch (*18*) and Almo et al. (*19*) examined substrate specificity requirements at the side chain subsite of AspAT. Via appropriate amino acid residue substitutions, they were successful in switching specificity from acidic amino acids and α-keto dicarboxylic acids to substrates with nonpolar or positively charged side chains. Toney and co-workers have extended the understanding of substrate specificity and reaction specificity in the alanine racemase (alanine racemase family) and dialkylglycine decarboxylase (α-family) systems (*15*) through detailed solution mechanistic and structural studies (*20–24*). These investigations provide new insight into the role played by stereoelectronic control in the determination of substrate fate regarding transamination, decarboxylation, or racemization. All of these studies and the available PLP enzyme structure data base confirm the structure–function relationships implied by Dunathan's hypothesis. Nevertheless, the role of protein conformational dynamics in substrate and reaction specificity is an emerging area of importance with respect to specificity and to the relationship between structure and function in PLP requiring enzymes. In this context, substrate interactions at the α-carboxylate subsite also appear to play an important role in triggering conformational transitions in the protein that are essential for catalysis in several PLP enzyme systems.

Inoue et al. (*25*) examined the effects of Lys substitution for R386 at the α-carboxylate subsite in *E. coli* AspAT. This

substitution was found to give a strong adverse effect on V_{max} and large increases in K_m, and it was concluded that substitution of Lys for Arg at position 386 is not structurally adequate to ensure the productive binding of substrates during catalysis. The replacement of R386 with Tyr or Phe reduced activity by a factor $>10^5$ (*26*) and appeared to stabilize an open conformation similar to wild-type enzyme.

While the above works are interesting they do not help in understanding the β-family of PLP enzymes because there is neither sequence homology between the α-family, the alanine racemase family, and the β-family of PLP enzymes nor similarity in substrate binding sites. In contrast to α-family enzymes, the α-carboxylate subsites of β-family enzymes all involve extensive H-bonding interactions between backbone and neutral side chain residues of a main chain loop but do not involve Coulombic charge−charge interactions to balance the formal negative charge on the α-carboxylate. In *O*-acetylserine sulfhydrylase from *S. typhimurium* (a β-family enzyme), binding of substrate to the α-carboxylate loop appears to induce a large conformational change in the enzyme, stabilizing the closed structure (*27*). Mutants of the α-carboxylate loop in cystathionine β-synthase (also a β-family enzyme) were found to significantly alter substrate reactivity and reaction specificity (*28*). The side reaction involving conversion of L-Ser to pyruvate and NH₃ via an α-aminoacrylate intermediate was enhanced by mutations in the loop, and mutations of residues that interact with the loop facilitated reaction of released α-aminoacrylate with the internal aldimine to give a covalent adduct with PLP. This same side reaction previously was reported to occur in amino transferases (*29, 30*) and several tryptophan synthase mutants (*31−34*).

In tryptophan synthase, the α-carboxylate binding loop, βL3, includes residues βT110, βG111, βA112, βG113, βQ114, and βH115 (Figure 1B) (*9*). This loop also is part of the communication (COMM) domain, a mobile but rigid domain involved in the allosteric signaling between the α- and β-active sites (*1, 5, 35−37*). H-bonding interactions between the substrate carboxylate and the βL3-loop residues include the backbone amide groups of βG111, βQ114, and βH115 and the side chain hydroxyl group of βT110. In this study, we report investigations of the roles played by loop residues βT110 and βQ114 in the catalytic activity and reaction specificity of tryptophan synthase through mutation. The side chain hydroxyl of βT110 is fixed in the correct position for H-bond formation with one oxygen atom of the substrate α-carboxylate and by an H-bond donated by the amide N−H of another loop residue, βG113 (see Figure 1B). The mutation βT110V was selected so that the disruption of this constellation of H-bonds resulting from replacement of the βT110 O−H by a CH₃ group could be investigated. The backbone amide N−H of βQ114 makes an H-bond to the other oxygen of the substrate carboxylate. The side chain of βQ114 is located in a niche that is formed on one side of the COMM domain. In this pocket, the side chain carbonyl oxygen atom OE1 of βQ114 is held in place by H-bonds to the side chain amide group of βN145 and the NH₂ nitrogen of the guanidinium group of βR148, and the side chain amide group of βQ114 is held by H-bonds to the carbonyl O of βG83 and to a water molecule (see Figure 1B) (*9*). These interactions anchor the COMM domain and may also influence the position of the catalytically essential βK87. The
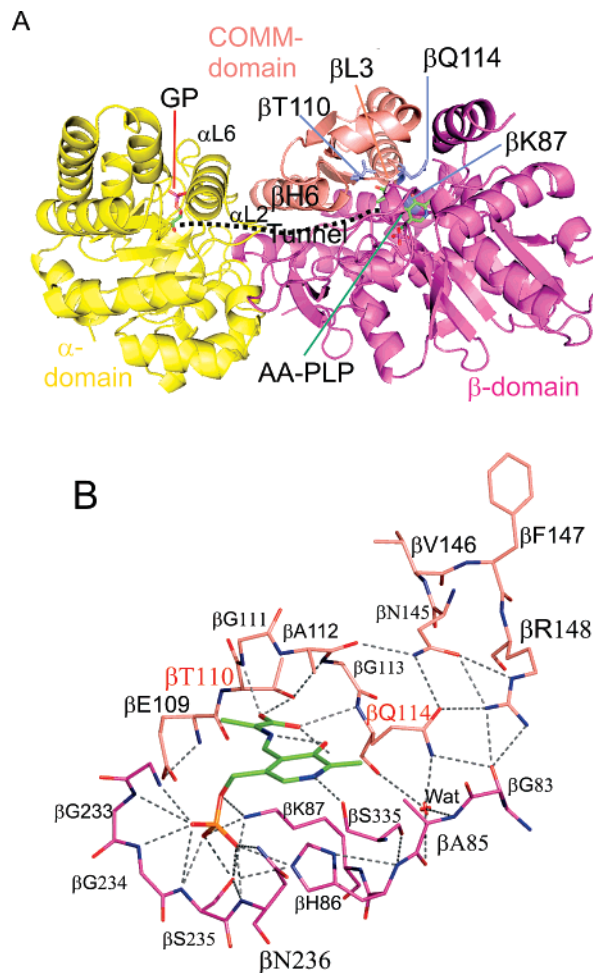

FIGURE 1: Structural overview of the closed conformation of the αβ-dimeric unit of tryptophan synthase with the α-aminoacrylate Schiff base bound to the β-site and D-glycerol-3-phosphate bound to the α-site (PDB 2J9X)(*9*). (A) The αβ-dimeric unit shown in ribbon representation (α-subunit yellow, β-subunit violet and pink, with the latter representing the COMM domain). Important structural elements, such as loops αL2 and αL6 in the α-subunit and helix βH6 of the COMM domain in the β-subunit, are labeled, as is loop βL3 (β110−β115) which interacts with the α-carboxylate of the bound substrate subsite residues. βL3 contains the two mutated residues, βT110 and βQ114, which are shown in cyan. The α-site ligand, D-glycerol-3-phosphate (GP), and the β-site ligand, the α-aminoacrylate Schiff base of PLP (AA-PLP), are shown as green sticks. The approximate location of the interconnecting ~25 Å-long tunnel is indicated by a dotted line. (B) Expanded view of the β-catalytic site showing the interactions of the α-aminoacrylate Schiff base (green sticks) with the protein, including the catalytic residues βK87 and βE109, and the interactions of the mutated residues βT110 and βQ114, labeled in red. Color coding is according to Figure 1A, with the COMM domain depicted in pink. H-bonds are indicated by dashed lines.

βQ114N mutation was selected to weaken or destroy these interactions and to potentially alter the motion of the COMM domain in the switch between open and closed states.

The βT110V and βQ114N mutations reveal important new aspects of the structural determinants for reaction specificity in tryptophan synthase. These structural determinants reflect subtle weak bonding interactions within the α-carboxylate subsite that are essential for biasing reaction in favor of one chemical path over competing pathways that lead to different fates, both for the substrate and for the coenzyme. We also show that structural perturbations at the L-Ser α-carboxylate subsite can result in unexpected consequences both for stage

I of the β-reaction and for allosteric signaling between the α- and β-sites. These results have important implications regarding the evolution of enzyme catalysis in the class of PLP enzymes that catalyze β-replacement and β-elimination reactions involving a reactive α-aminoacrylate external aldimine intermediate.

MATERIALS AND METHODS

Materials. L-Ser, 2-aminophenol (2-AP), serinol, and β-mercaptoethanol were purchased from Sigma as the highest purity materials available and used without further purification. Indoline was purified as previously described (*38*). The procedures for the synthesis and purification of *N*-(4′-trifluoromethoxybenzenesulfonyl)-2-aminoethyl phosphate (F9) and its characterization as an α-site ligand for tryptophan synthase are described elsewhere (*39*).

The 1.7 kb EcoRI/HindIII fragment of pSTB7 (*40*) (gift from R. Bauerle) was subcloned into the EcoRI and HindIII site of pUCBM20 (Boehringer). This yielded plasmid pUC1. For mutagenesis, the 1.1 kb EcoRI/EcoRV fragment of pUC1 was excised and inserted into the EcoRI and EcoRV site of pUCBM20 to construct pTS-1.1RI/RV. The mutation at codon 114 of the trpB gene was introduced by a PCR-based method (*41*) using pTS1.1RI/RV as template and the following oligonucleotides:

TSA (5′-GACCATGATTACGAATTCGGCGGCATG-3′)
TSB (5′-GCCAAGCTTCCATGGGATATCGTGTAC-3′)
Q114N.1 (5′-ACCGGCGCCGGT<u>AAC</u>CACGGCGTCGCC-3′)
Q114N.2 (5′-GGCGACGCCGTG<u>GTT</u>ACCGGCGCCGGT-3′)

(site of mutation underlined)

The nonmutated 1.1 kb EcoRI/EcoRV fragment of pUC1 was replaced with the 1.1 kb PCR product containing the mutation to generate plasmid pTS-Q114N. The 1.7 kb EcoRI/HindIII fragment from pTS-Q114N was recloned into EcoRI/HindIII digested pSTB7 and the resulting plasmid termed pSTB7-βQ114N was transformed into the *Escherichia coli* CB149 strain lacking the trp operon.

The threonine to valine mutation at codon 110 (T110V) of the trpB gene was introduced accordingly using the following oligonucleotides:

T110V.1 (5′-GATTATCGCTGAA<u>GTT</u>GGCGCCGGT-CAG-3′)
T110V.2 (5′-CTGACCGGCGCC<u>AAC</u>TTCAGCGATAA-TC-3′)

Subsequent cloning of the mutated gene was performed as described above.

Purification of the wild-type and mutant tryptophan synthase species from *Salmonella typhimurium* was performed as described previously (*40, 42, 43*). In contrast to the preparations of the wild-type and βT110V mutant enzymes that yield yellow colored proteins, βQ114N purification yields a protein solution of reddish color. Unless otherwise stated, all solution studies were carried out in 100 mM NaCl to keep the enzyme in the Na$^+$ form (*38, 44*), all of the reactions were run at 25 °C in 50 mM TEA buffer pH 7.8. Enzyme concentrations were typically 20−30 μM $\alpha\beta$-sites.

Static and Stopped-Flow Kinetic UV/vis Absorbance and Circular Dichroism Measurements. Absorbance spectra,

stopped-flow kinetic measurements, and activity measurements were performed as described previously (*45, 46*). Kinetic time courses were fitted by nonlinear least-squares regression analysis using the software Peakfit (version 4, Jandel Scientific) to a sum of exponentials according to eq 1

$$\emptyset_t = \emptyset_\infty \pm \sum_i \emptyset_i \exp(t/\tau_i) \tag{1}$$

where $\emptyset_t$ is the absorbance or fluorescence at time t, $\emptyset_\infty$ is the final value of the absorbance or fluorescence, and $\emptyset_i$ is the absorbance or fluorescence due to the ith relaxation, and $1/\tau_i$ corresponds to the observed rate for the ith relaxation. Circular dichroism (CD) measurements were performed on a Jobin-Yvon Dichrograph Mark V spectrometer.

^{1}H NMR Spectroscopy. The preparation of samples and data collection for analysis of the 426 nm species was conducted as previously described (*33*).

Crystallization, Complex Formation, Diffraction Data Collection, and Refinement. The βT110V and βQ114N tryptophan synthase mutants were crystallized as previously described for the wild-type enzyme (*1*). Crystals of the βQ114N mutant were reddish in color. Attempts to form complexes were undertaken by soaking native crystals for 10 min in a solution containing 90 mM bis-tris-propane pH 7.8, 150 mM NaCl, 15% (w/v) PEG 8000, 20% glycerol, and 10 mM of indolepropanol phosphate (IPP; βT110V only) in the presence or absence of 200 mM L-Ser. No complexes were obtained with the βT110V mutant as judged from the electron density obtained from soaked crystals (data not shown). For the βQ114N mutant, soaking with L-Ser in the absence of an α-site ligand was also performed overnight. Diffraction data were collected either at the National Synchrotron Light Source (NSLS; Brookhaven National Laboratory, New York) or the Swiss Light Source (SLS; Paul-Scherrer Institute, Villingen, Switzerland) with the crystals kept at 100 K. Diffraction data were processed with the XDS suite of programs (*47*), see Table 1. The IPP complex with wild-type E(Ain) (PDB code 1QOP) was used as a starting model for structure determination. To reduce model bias, loops αL2 and αL6, IPP, PLP, the sodium ion, and all water molecules were omitted. For each structure, the initial model was divided into three parts (α-subunit, COMM domain (*1*), and the core of the β-subunit) that were subjected to rigid body and simulated annealing refinement by CNS 1.1 (*48*).

In the structures obtained for βT110V and βQ114N, loop αL6 is disordered and was therefore omitted in the refinement, while αL2 was included. Most water molecules were placed automatically using the CNS Waterpick routine. Structures were superimposed with the program "O" (*49*) and Xfit (*50*) using all C$_\alpha$ atoms for each pair of structures except those belonging to loop αL2, loop αL6, and the COMM domain.

Quantum Chemical Calculations of Pyridoxal Phosphate Intermediates. To support the assignment of the optical absorption spectra, the energies of the electronic transitions of the intermediates of the β-reaction in the mutant were calculated using *ab initio* quantum chemical methods. According to experimental observations, the dephosphory-lated analogue exhibits absorption properties very similar to

Table 1: Crystallographic Data

complex	$^{\beta T110V}E(Ain)$	$^{\beta Q114N}E(CPII)$
PDB code	2J9Z	2J9Y
crystal parameters		
space group	*C2*	*C2*
unit cell	182.8, 59.9, 67.6	182.7, 60.7, 67.4
(a, b, c [Å], β [deg])	94.40	94.83
data collection		
beamline	X12C	X10SA
X-ray source	NSLS	SLS
wavelength [Å]	1.0	0.905
data statistics		
resolution [Å]	20−1.8	20−1.7
no. of observations/	172916/64747	247781/80056
unique reflections		
completeness (total/high) [%][a]	95.5/90.2	98.7/98.8
$\langle I/\sigma(I)\rangle$ (total/high)[a]	7.1/2.0	9.0/3.8
R_{sym},(total, high)[a,b]	11.6/33.0	8.6/34.4
refinement statistics		
resolution range [Å]	19.85−1.8	19.45−1.8
refinement program	CNS 1.1	CNS 1.1
included amino acids	A 1−177	A 1−178
	A 194−267	A 194−267
	B 2−393	B 2−394
no. of protein atoms	4785	4875
no. of waters	574	564
no. of ligand atoms	15	21
no. of Na$^+$ ions	1	1
R_{work}, R_{free} [%][c]	18.7/21.8	22.8/26.3
rms deviation for bonds/	0.006/1.34	0.006/1.25
angles [Å/deg]		

[a] Completeness, R_{sym}, and $\langle I/\sigma(I)\rangle$ are given for all data and for the highest resolution shell. Resolution shells are: 1.8−1.9 (T110V), 1.7−1.8 (Q114N). [b] $R_{sym} = \Sigma|I - \langle I\rangle|/\Sigma I$. [c] $R_{work} = \Sigma|F_{obs}| - k|F_{calc}|/\Sigma|F_{obs}|$. The calculation of R_{free} involved 5% of randomly chosen reflections.

that of compound III obtained in the enzymatic reaction (*29*). Therefore, to reduce the size of the model system, the molecules without the phosphoryl group were used for the calculations. The geometries of the model compounds were optimized by the B3LYP/6-31G(d) method (*51*, *52*). Energies of the first $\pi-\pi^*$ electronic transition were estimated as a difference between diagonal elements of the second-order MCQDPT Hamiltonian (*53*) with the state-averaged CASSCF(2,2) zero-order wave function accounting for the excitations within the active space containing π and π^* MOs. For all considered molecules, by the inspection of the CI−SD wave functions calculated for the five low-lying electronic states, the π and π^* MOs were identified to be HOMO and LUMO of the Hartree−Fock reference electronic configuration. The PC GAMESS 6.4 version (*54*) of the GAMESS quantum-chemical package (*55*) was used for calculations.

RESULTS

The βT110V Mutant Exhibits a Perturbed Absorption Spectrum. The spectrum of $^{\beta T110V}E(Ain)$ ($\lambda max = 404$ nm) is blue-shifted from the wild-type form by approximately 10 nm (Figure 2A). This shift in the internal aldimine spectrum implies that the mutation causes a perturbed microenvironment of the PLP chromophore.

Reactions of βT110V with L-Ser and Serinol. The reaction of either L-Ser or serinol with the βT110V mutant results in a shift of the PLP spectrum to $\lambda_{max} = 410$ nm and increases the absorbance at 330 nm (Figure 2A). The predominating species formed appear to be the respective external aldimines. Very little, if any, E(A-A) is formed with L-Ser, and there is no indication that the serinol external aldimine undergoes

β-elimination to give an external aldimine comprised of PLP and 2-aminopropenol. Consequently, the shifted spectra indicate that the mutation perturbs the microenvironment of the PLP chromophore, and that the βT110V mutant reacts with L-Ser or serinol to give Schiff base species with absorption bands that are also perturbed in comparison to the wild-type enzyme (*10*, *56*, *57*). No evidence was found indicating that serinol reacts with the wild-type enzyme.

Titration of the βT110V mutant with L-Ser indicates that the binding and reaction of L-Ser to form the E(Aex$_1$) species is impaired, giving a considerably weakened interaction (Figure 2B, $K_{Dapp} = 90$ μM for the wild-type enzyme while $K_{Dapp} = 27$ mM for the mutant). The titration of the βT110V mutant with serinol indicates that the interaction with this analogue is even weaker, and a meaningful apparent dissociation constant was not determined. Upon addition of L-Ser, both the wild-type and βT110V mutant enzymes show a decrease in the CD signal centered around 410 nm, indicating formation of E(Aex$_1$), a species with a much lower ellipticity than the E(Ain) (Figure 2C). In the case of the wild-type enzyme, there is also a large negative band in the 330 nm region indicating formation of E(A-A), while in the mutant there seems to be only a slight decrease at that wavelength, which may correspond to a small amount of E(A-A). This is consistent with the L-Ser titrations in the absence of the α-site ligand (ASL) F9 (data not shown). These findings indicate that the βT110V mutation influences both the substrate specificity and reaction specificity.

The Influence of F9 on the Reaction of the βT110V Mutant with L-Ser and 2-AP. In wild-type tryptophan synthase, the reaction of 2-aminophenol (2-AP) with the wild-type α-aminoacrylate intermediate gives a stable quinonoid species with
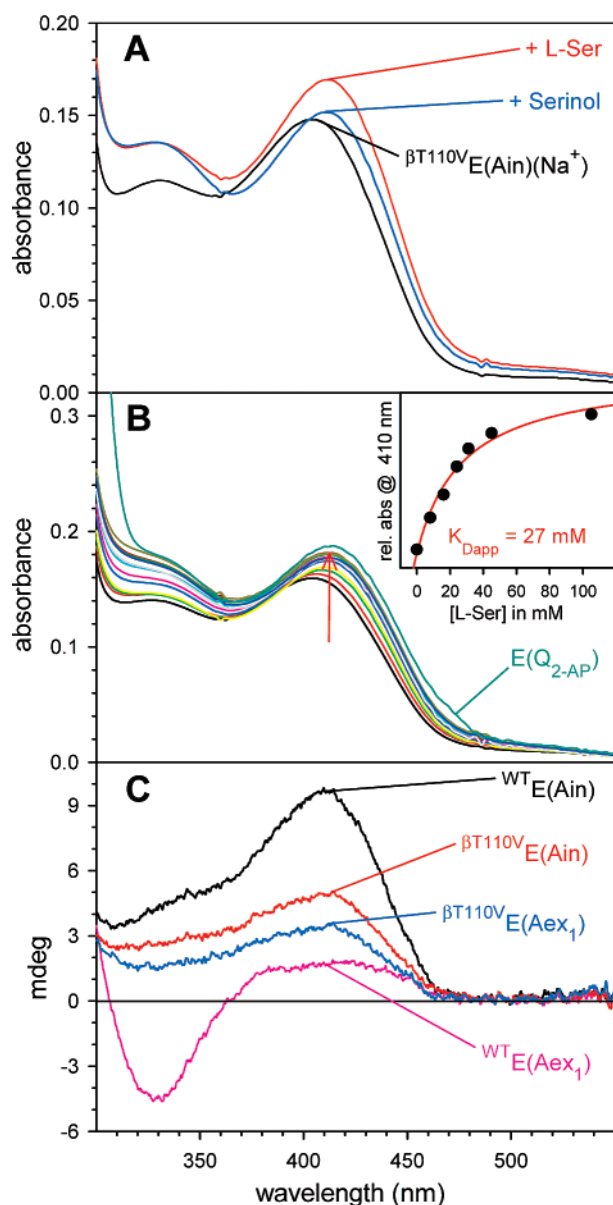
FIGURE 2: Comparison of the UV/vis and CD spectra of the wild-type enzyme and of the βT110V mutant. (A) Reaction of $^{\beta T110V}$E-(Ain) ($\lambda_{max} = 404$ nm) with L-Ser and serinol. (B) Titration of $^{\beta T110V}$E(Ain) with 0−250 mM L-Ser in the presence of 200 μM F9. Following the L-Ser titration, 600 μM 2-AP was added. In the presence of 2-AP, a small amount of quinonoid accumulates. (C) CD spectra of the reaction of βT110V and wild-type with L-Ser in the presence of CsCl. The wild-type enzyme shows a decrease in the signal centered around 410 nm and a large negative band in the 330 nm region; the mutant gives only a slight decrease around 330 nm and an increase in the 410 nm region.

$\lambda_{max} = 466$ nm and $\epsilon_{max} > 60\,000$ M^{-1} cm^{-1} (spectrum not shown). Consequently, the 2-AP reaction provides a sensitive assay for the formation of the α-aminoacrylate external aldimine. The binding of ligands to the α-site, for example α-D,L-glycerol-phosphate (GP) or F9, further stabilizes the 2-AP quinonoid species. Addition of 2-AP to the mutant in the presence of saturating L-Ser gives no detectable quinonoid species. Repetition of this experiment in the presence of F9 appears to give a trace amount of quinonoid species, corresponding to at most 1−2% of enzyme sites (Figure 2B). No evidence of the formation of a quinonoid-like species with 2-AP in either the presence or the absence of F9 was

Table 2: Comparison of the Steady-State Parameters of the Wild-Type Enzyme to the βT110V Mutant in the Presence of NaCl

reaction type	wt (s^{-1})	βT110V (s^{-1})	wt/βT110V
α	0.091	0.034	~3
β	7.0	0.003	~2300
α + 2 mM F9	0.012	0.006	~2
β + 2 mM F9	0.72	−	−

found for the serinol complex. These results indicate the mutation has modified the reaction specificity of the enzyme.

Steady-State Kinetic Activities of the βT110V Mutant. Steady-state kinetic measurements show that the α-reaction of the mutant is slightly impaired by the mutation (decreased by ~1/3), whereas the β-reaction is strongly impaired (decreased by ~1/2300) (Table 2). The rate of production of pyruvate is slow compared to the rate obtained with the wild-type enzyme under the same conditions. This result is consistent with the absence of a quinonoid species and thus confirms that the mutant makes very little E(A-A), demonstrating that the mutant has an altered reaction specificity.

Structure of the βT110V Mutant and Effects of the Mutation on the β-Site. To investigate the structural basis for the kinetic impairments exhibited by the βT110V mutation, an effort was undertaken to determine the structures of the internal aldimine species and the L-Ser complex of the mutant in the absence and the presence of ASL. Interestingly, none of the mutant crystals that were soaked with IPP displayed electron density for the α-site ligand and therefore were not refined beyond the first refinement step. Since none of the expected E(Aex$_1$) complexes prepared in the presence of an excess of L-Ser showed electron density for an external aldimine but only for an E(Ain)-like co-valently bound PLP at the β-active site, refinement of those structures was stopped also after the first cycle.

All attempts to prepare complexes of the β-domain, whether soaked in the presence or absence of IPP or L-Ser, respectively, gave highly similar structures (deviations are within experimental error) and display an internal aldimine state with an unoccupied α-active site. Comparing the E(Ain) mutant without ASLs with the wild-type structure (PDB code 1KFK), several structural differences can be observed.

In the wild-type protein, the subsite that binds the α-carboxylate of the substrate L-Ser is formed by loop βL3 (see Schneider et al. (*1*) for description of the structural elements, loops, helices, and domains of tryptophan synthase). In this loop, the hydroxyl group of βT110 is engaged in a H-bond network with the backbone amides of βA111 (3.1 Å) and βG116 (3.1 Å), and WAT155 (2.9 Å) which is coordinated by the amide group of βH115, thereby stabilizing the position of loop βL3 (Figures 1 and 3). The loss of this interaction in the βT110V mutant leads to an expansion of the loop region (βA108−βH115) that affects the surrounding structural elements of the β-domain and thus impacts enzymatic function, allosteric communication, and substrate/reaction specificity.

The βT110V Complexes Exhibit a Distorted Allosteric Interface. As a result of the mutation-induced changes in βL3, all regions within the β-subdomain that were previously attributed to the allosteric network that conveys signals during intersubunit communication at different steps of the enzymatic reaction (*1, 9, 33−36, 39, 58−60*) were found to be changed. βI132−βF185, the region preceding and includ-
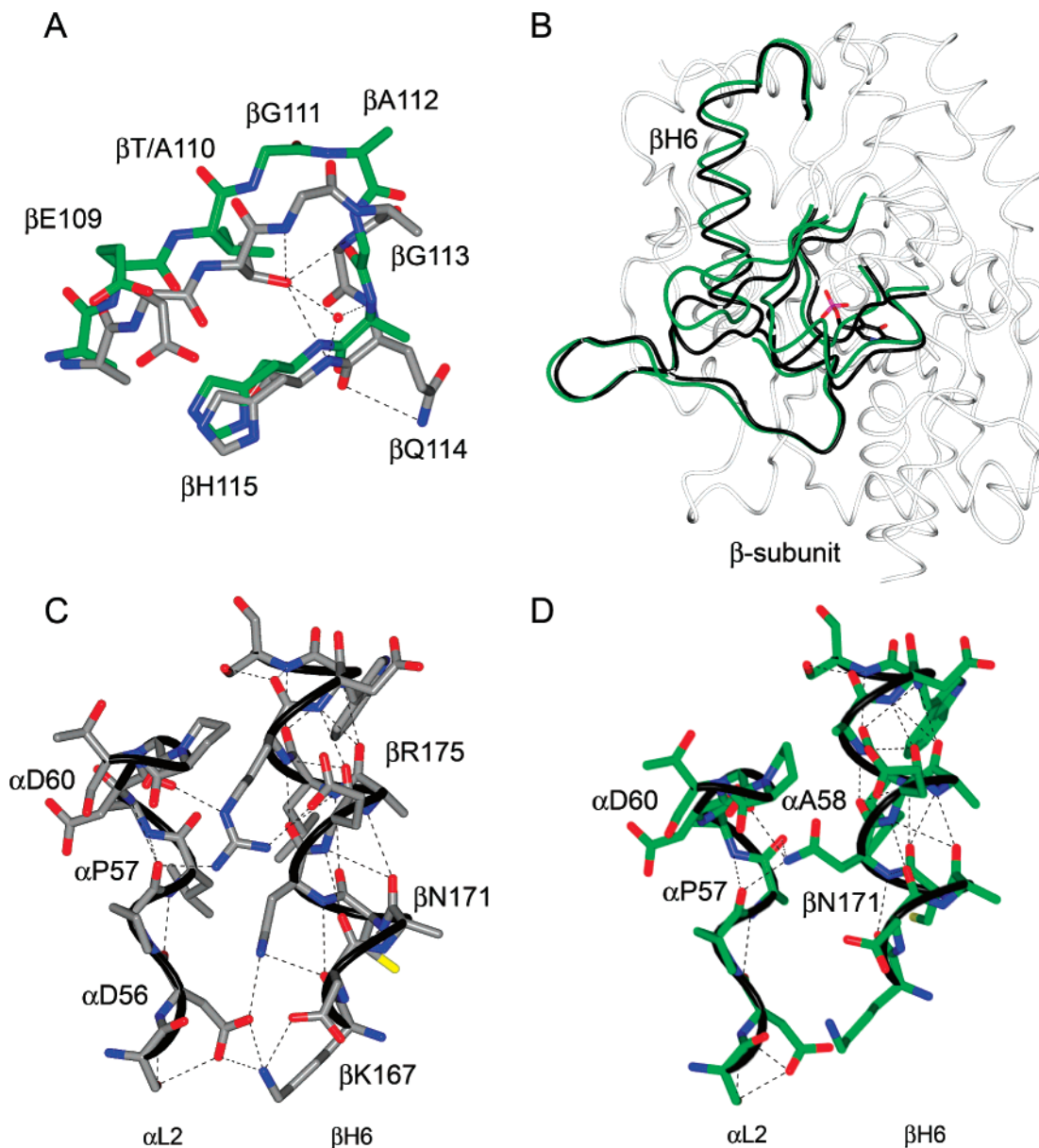
FIGURE 3: Structural consequences of the βT110V mutation in tryptophan synthase. (A) Structural details of βL3. Superposition of the wild-type ASL-free E(Ain) state (PDB code 1KFK, gray) with the $^{\beta T110V}$E(Ain) mutant complex (green). Residues of βL3 are labeled; dashed lines indicate H-bonds in the wild-type protein. Those side chains of the mutant that were not visible in the electron density were replaced by alanines. (B) Structural superposition of the β-subdomain of the E(Ain) structure and the βT110V mutant complex in worm representation. The mutant structure was superimposed on the E(Ain) complex as in (A) (white and black). Only those regions that were found to change significantly in the mutant structure are displayed (green) and the same area highlighted for the wild-type protein (black) for contrast and clarity. (C and D) Details of the intersubunit interface of tryptophan synthase. Shown are the interacting side chains and H-bonds between αL2 and βH6 of wild-type E(Ain) (C) and $^{\beta T110V}$E(Ain) (D). The side chains are labeled and color-coded as in A. The backbone of the α loop and the β helix are displayed in black for clarity.

ing the βH6 helix (βE165−βH181), and to a minor degree βP285−βY298 are massively changed by an altered set of intramolecular H-bonds within this region (Figure 3B). Consequentially, the intersubunit interface between αL2 and βH6 that conveys signals between the α- and the β-sites (*1, 5, 9, 39*) is structurally changed by the movement of the βH6 helix. In the corresponding wild-type enzyme structure (PDB code 1KFK), the interface consists mainly of the interactions between the side chains of βK167, βN171 and βR175, and αD56, αP57, and αD60 within αL2 of the α-subdomain (Figure 3C). In the βT110V mutant, the interface consists only of the interactions of βAsn171 with the main chain carbonyl groups of αP57, αA58, and αD60

(Figure 3D). As a consequence of the lost contact between βR175 and αD60, the arginine side chain becomes mobile and thus is not observed in the electron density of the structure. These results demonstrate the structural origins of the modified specificity exhibited by the mutant.

The βQ114N Mutant Exhibits an Unusual Absorption Spectrum. To investigate the impact of the amino acid at position β114 on the enzymatic reaction of tryptophan synthase, βGln114 was replaced by Asn. The βQ114N mutant is reddish, with UV/vis absorption bands located at ∼410 nm and ∼500 nm (Figure 4A). Analysis of these bands using lognormal curves (*61*) to decompose the spectrum indicates that the band maxima occur at λ_{max} 414 and 506
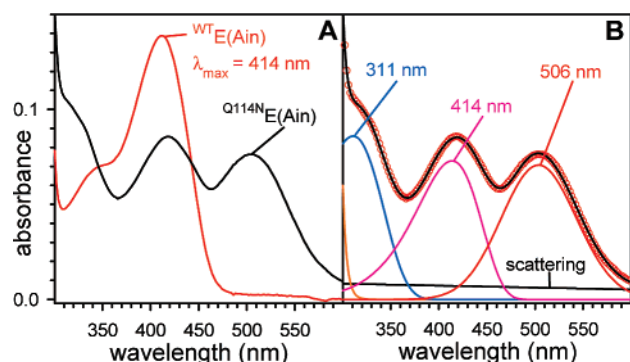
FIGURE 4: (A) Comparison of the wild-type internal aldimine, E(Ain) (black), with the βQ114N mutant enzyme, E(Ain) (red). (B) Lognormal deconvolution (*61*) of the spectrum of the βQ114N internal aldimine, E(Ain), into peaks with λ_{max} = 311, 414, and 506 nm. Red circles, experimentally measured spectrum; solid black line, fitted spectrum.

nm, respectively (Figure 4B). Assuming the extinction coefficient for the 414 species is comparable to the 414 nm species of the wild-type enzyme, the 506 nm peak of the perturbed E(Ain) spectrum of the mutant accounts for approximately 35% of total sites.

Reaction of the βQ114N Mutant with L-Ser. Reaction of the βQ114N mutant with L-Ser gives a ~424 nm band that forms relatively rapidly (within 10 s). There is no change in the 506 nm spectral band during this time period. Time-resolved spectra for the 10 to 900 s interval show that the 424 nm band disappears with concomitant formation of a ~320 nm species, whereas the 506 nm band remains unchanged (Figures 5A and B). Since the amplitude and the position of the maximum of the 506 nm band do not change during the course of the reaction, while the 424 nm band is almost completely converted to the 320 nm band after 900 s, it appears that there are at least two species of enzyme-bound PLP present after 10 s, a 424 nm species and a 506 nm species. The 424 nm species is reactive, converting to a ~320 nm species over the 900 s time interval shown in Figure 5. The 506 nm species is unreactive toward L-Ser and corresponds to the 506 nm species found in the isolated and purified enzyme. Upon completion of the conversion of the 424 nm species to the ~320 nm species, all activity of the βQ114N mutant in the β- and $\alpha\beta$- reactions has disappeared, and the β-site appears to have been inactivated. The activity of the βQ114N mutant in the β-reaction (the reaction of L-Ser and indole to give L-Trp) decays away, following the same kinetic time course as the formation of the 320 nm species. The coupled assay for pyruvate (using lactate dehydrogenase and NADH) shows that during the initial 900 s time period, there is significant conversion of L-Ser to pyruvate. The time course for pyruvate formation (data not shown) indicates that as the 424 nm species is converted to the ~320 nm species, the rate of formation of pyruvate also decreases to zero. Owing to the small extinction coefficient of pyruvate, the amount produced makes only a minor (~10%) contribution to the absorbance at 320 nm. Comparison of the yield of pyruvate formation to the fraction of inactivation indicates that the partitioning between these paths appears to favor pyruvate formation over inactivation by a ratio of about 50:1.

Upon incubation with excess L-Ser for ~ 24 h, all of the species with λ_{max} ~ 320 nm converts to the 506 nm species.
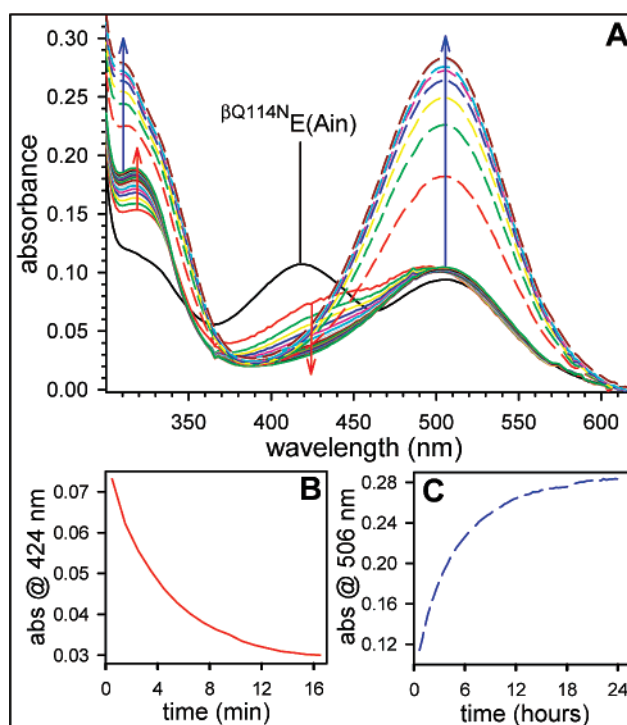

FIGURE 5: Panel A shows the reaction of the βQ114N E(Ain) with L-Ser. The time-resolved spectra show the disappearance of a species with λ_{max} ~ 424 nm in favor of an intermediate with λ_{max} ~ 320 nm formed within the initial 15 min. This spectral change is followed by appearance of a species with λ_{max} = 506 nm that occurs on a 24 h time scale. Panel B shows the disappearance of the 424 nm species, while panel C shows formation of the 506 nm species.

Activity measurements establish that the β-site of this species also is catalytically inactive. These results strongly suggest that during expression or purification, a fraction of the βQ114N mutant reacts with L-Ser present in the growth media and/or the cells to give the 506 nm species. When incubated with L-Thr, no changes in the absorption spectrum were observed, indicating that no reaction occurs with this amino acid and that the spectral changes observed with L-Ser are indicative of a specific reaction of the mutant with substrate, L-Ser. These findings demonstrate that the βQ114N mutation strongly alters the reaction specificity of the enzyme.

Reaction of βQ114N with L-Ser and Nucleophilic Analogues of Indole. The reaction of βQ114N with L-Ser and either β-mercaptoethanol, indoline (*8, 62*), or 2-AP gives quinonoid species exhibiting absorption bands that differ from those formed with the wild-type enzyme (Figure 6). Analysis of these spectra indicates that there is no change in the amount of the 506 nm species present. The quinonoid formed with β-mercaptoethanol gives a maximum at 492 nm (vs 466 nm for wild-type enzyme), indoline gives a maximum at 486 nm (wild-type 468 nm), and 2-AP gives a maximum at 484 nm (wild-type 466 nm).

Rapid kinetic studies (data not shown) demonstrate that the reaction of indoline with the βQ114N α-aminoacrylate shows a rapid formation of the mutant quinonoid species, $^{\beta Q114N}$E(Q)$_{indoline}$, similar to that exhibited by the wild-type enzyme (*3, 6, 8, 62, 63*). With the wild-type enzyme, it has been shown that when an α-site ligand is bound, the reaction is greatly slowed, indicating that access to the β-site via the
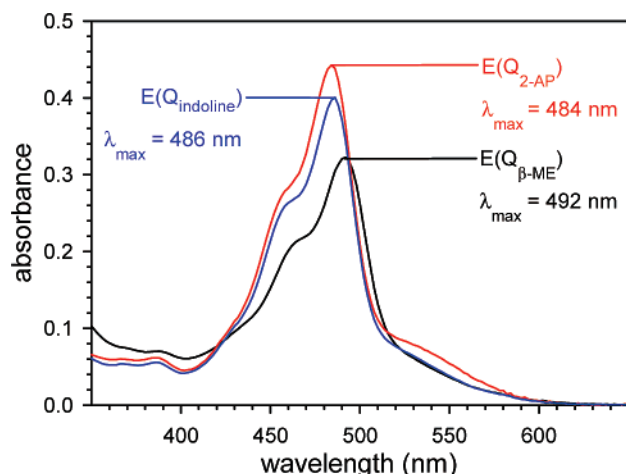
FIGURE 6: Reaction of the βQ114N E(Ain) with L-Ser and either 2-aminophenol, indoline, or β-mercaptoethanol, giving, respectively, E(Q)$_{2-AP}$, E(Q)$_{indoline}$, or E(Q)$_{\beta-ME}$.

α-site and the interconnecting tunnel is blocked by the conversion of the α-site to the closed conformation. These studies confirm that the βQ114N α-aminoacrylate acts similarly when the α-site is occupied by F9, indicating that allosteric communication and the switching between open and closed states is not drastically altered by the mutation.

Steady-State Catalytic Activities for the α-, β-, and $\alpha\beta$-Reactions of βQ114N. At relatively short incubation times with L-Ser, the βQ114N mutant exhibits catalytic activities in the α-, β-, and $\alpha\beta$-reactions that are similar to the wild-type enzyme (Table 3). This comparison shows that the mutant preparation, isolated and purified by the same procedure employed for the wild-type enzyme, is approximately 35% less active than the wild-type enzyme. This decrease in activity appears due to the presence of approximately 35% of the enzyme as the inactive, 506 nm species. The remaining protein appears to have essentially full, wild-type-like, catalytic activity. In the Na$^+$ form of the wild-type enzyme, reaction of L-Ser at the β-site to give E(A-A) triggers an allosteric interaction that causes a $\sim$30-fold activation of the α-site (*2, 4, 64*). Conversion of the mutant to the 506 nm species by incubation with L-Ser for 24 h reduces the α-site activity only slightly (Table 3). The $\alpha\beta/\alpha$ activity ratio measures the activation of the α-reaction resulting from the allosteric signaling arising from E(A-A) formation at the β-site (*2, 65*). The 29-fold activation of the α-reaction activity exhibited by the mutant enzyme preparation measured immediately after reaction of L-Ser (Table 3) demonstrates that allosteric interactions between the α- and β-sites are essentially intact in the unmodified mutant.

Characterization of the L-Ser Inactivated βQ114N Mutant. The formation of a 426 nm PLP species via a $\sim$320 nm species during the reaction of L-Ser with the βQ114N mutant (Figures 5 and 7) is similar to the behavior of several other tryptophan synthase mutants (but not the wild-type enzyme) (*31–34*) and to the behavior of at least two other PLP enzymes (*29, 30*). Such a 426 nm species (designated here as compound III, Scheme 3) has been isolated previously and shown to be due to a covalently modified PLP produced in a side-reaction believed to involve the transient species, α-aminoacrylate, released within the catalytic site (*29–34*) (Scheme 3). In these systems, the rate of formation of the

426 nm species is increased by treating the 320–340 nm species with NaOH.

To further characterize the enzyme species formed during the incubation of L-Ser with the mutant followed by treatment with NaOH, the following experiments were performed. Deconvolution analysis shows that addition of NaOH to the βQ114N mutant results in a mixture of 390 and 426 nm peaks (Figure 7A). The 390 nm species was shown to be the enzyme-free PLP hydrate, a well-documented species ($\lambda_{max} = 390$ nm) (*61*) (Figure 7B). The 426 nm species has been previously isolated and identified as a covalent product formed with PLP, a consequence of a side-reaction previously seen with tryptophan synthase and at least two other PLP-dependent enzymes (*29–34*). The ^{1}H NMR spectrum of the 426 nm species isolated after the reaction of NaOH with the βQ114N mutant is indistinguishable from said species isolated previously (*33, 34*). Repetition of the NaOH treatment following incubation of the mutant with L-Ser for 24 h gives only the 426 nm species (Figure 7C). These results give three conclusions: (a) a fraction of the βQ114N mutant as isolated and purified behaves normally, releasing PLP at high pH, (b) a second fraction of the βQ114N mutant exhibits abnormal behavior suggesting that some of the pre-existing enzyme-bound PLP is covalently modified, and (c) incubation with L-Ser for long time periods ($>$24 h) results in a series of reactions that generate the 506 nm species. Treatment of this species with NaOH gives a 426 nm species previously identified as compound III. These findings demonstrate that the mutation causes structural and catalytic changes that alter the fate of the substrate and the coenzyme.

Theoretical Quantum Mechanical Calculations of Absorption Maxima of PLP-Related Species Formed by the βQ114N Mutant in Stage I of the β-Reaction. To further assess the nature of the 506 nm species, quantum chemical calculations of the theoretical absorption maxima of different PLP intermediate analogues were performed. The structures of the models together with the calculated and experimental absorption maxima, λ_{max} are presented in Table 4. The first $\pi-\pi^*$ transition in the compounds can be assigned to the HOMO–LUMO. The calculated λ_{max} values are in good agreement with experimentally determined ones, supporting the assignment. The calculated absorption maximum of the PLP analogue $\lambda_{max\ calc} = 397$ nm compares well with the experimental value of $\lambda_{max} = 390$ nm. Also, the calculated value ($\lambda_{max\ calc} = 420$ nm) for the external aldimine modeled as the methylamine imine analogue fits nicely with the experimental value of 424 nm for the enzyme-bound serine external aldimine. As previously assigned (*66, 67*), the calculated value matches best with a model that contains a protonated pyridine-nitrogen and a deprotonated 3-hydroxyl group.

The discrepancy between calculated and experimental values is somewhat larger for compound I. For this calculation, the molecular model for compound I was locked in a conformation by an intramolecular H-bond between the carboxylic acid group and the pyridine ring phenolate O$^-$. This interaction was chosen to mimic the expected H-bonding interaction analogous to the H-bond observed between the βAsn114 side chain amide NH and the phenolate O$^-$ in the mutant complex assigned as compound II (Figure 8). We propose that this H-bond has special significance in the mutant system. In the wild-type enzyme, the corresponding

Table 3: Comparison of the Steady-State Parameters of the Wild-Type Enzyme to the βQ114N Mutant

α (s^{-1})			β (s^{-1})		$\alpha\beta$ (s^{-1})		$\alpha\beta/\alpha$	
wt	βQ114N	βQ114N 24h[a]	wt	βQ114N	wt	βQ114N	wt	βQ114N
0.1	0.096[b]	0.05	7.4	6.8[b]	3.0	2.8[b]	30	29[b]

[a] After incubation with L-Ser for 24 h. [b] Values adjusted assuming that only 65% of the mutant protein is active, see Figure 4.
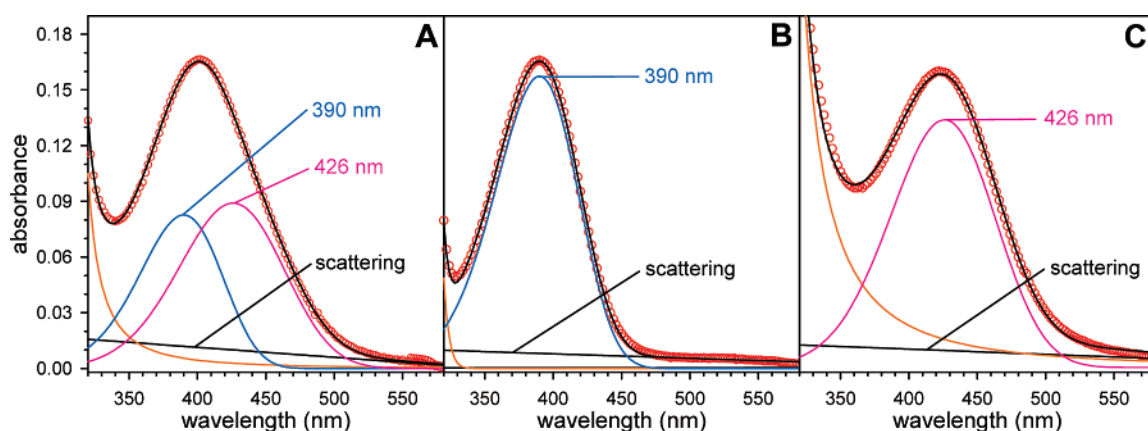

FIGURE 7: Comparison of the effects of NaOH on the wild-type and βQ114N mutant enzymes. (A) Addition of NaOH to the βQ114N mutant E(Ain) results in a broad envelope with an apparent λ_{max} at 402 nm. This spectrum can be decomposed via lognormal fitting (*61*) into a mixture of species with λ_{max} = 390 and 426 nm. (B) Addition of NaOH to wild-type, E(Ain), such that a pH of ~13 is reached, results in a species with a λ_{max} = 390 nm. (C) Addition of NaOH to the βQ114N mutant, after incubation for 24 h with L-serine, results in a species with a λ_{max} = 426 nm. Panels A−C: red circles, experimentally measured spectrum; solid black line, fitted spectrum.

Scheme 3: Proposed Mechanism for Covalent Inactivation of the βQ114N Mutant and the Possible Identities of the Intermediates Detected via UV/vis Spectroscopy
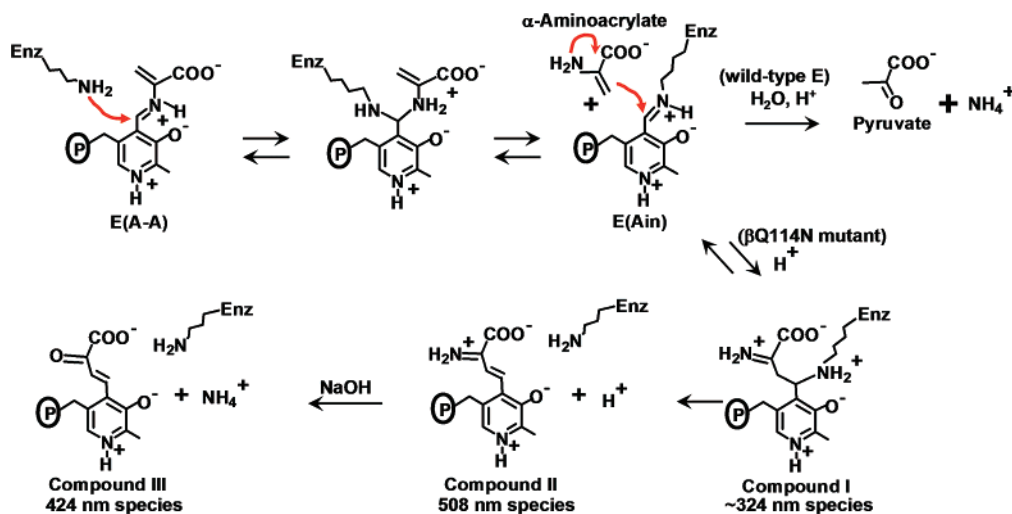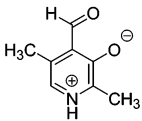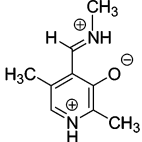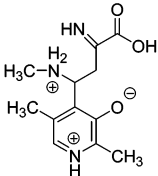

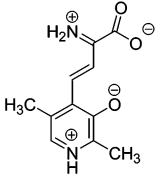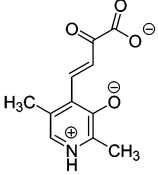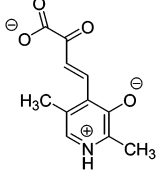βGln114 does not form an H-bond with the phenolate O$^-$ of the cofactor and instead in the closed β-subunit structure, (*9*) it is folded away from the coenzyme and makes H-bonds to βG83, βN145, βR148, and a water molecule. The altered side chain orientation and the new H-bond observed in the β114N mutant is likely to be essential for the altered chemistry performed by the mutant, resulting in increasing either the yield or the stability of compound I. Compounds II and III have essentially isosteric molecular frameworks, and thus, cannot be distinguished from each other in the electron density maps for compound II. The different UV/vis absorption properties of compounds II and III (Figures 4, 5, 7, and Scheme 3) are caused by different protonation patterns resulting from replacement of the iminium ion of compound II by the carbonyl of compound III, different extents of π-electron delocalization, and by changed in-

tramolecular interactions resulting from the different orientations and properties of the functional groups with respect to each other. For example, compound II is likely to occur in a zwitterionic state, while compound III is a carboxylate anion (viz. Scheme 3 and Table 4), and the positively charged iminium ion of compound II facilitates more charge delocalization at the phenolate O$^-$ than does the corresponding carbonyl of compound III. Compound III dissociates from the binding pocket after the alkaline treatment (*29, 33, 34*). In solution, the rotation of the fragment around the C$_\alpha$−C$_\beta$ bond is not restrained, yielding two rotamers with calculated maxima at 407 and 456 nm, respectively, for comparison with the observed λ_{max} = 426 nm (Table 4).

Structural Analysis of the βQ114N Mutant. In order to identify the structural basis of the kinetic and spectroscopic effects measured for the βQ114N mutant, the structures of

Table 4: Calculated Absorption Spectrum Maxima of PLP Intermediate Analogues

PLP intermediate analogue	Structure formula	$\lambda_{\text{max calc}}$ ($\lambda_{\text{max exp}}$)[a]
Free PLP analogue		397 nm (390 nm)
Protonated methylamine imine PLP external aldimine analogue		420 nm (424 nm)
Compound I		362 nm (320 nm)
Compound II		532 nm (506 nm)
Compound III		407 nm (426 nm)
Compound III		456 nm (426 nm)

[a] $\lambda_{\text{max exp}}$ measured for free and bound species identified in Figures 4, 5, 7, and Scheme 3).

the mutant in the absence and presence of L-Ser were determined to a resolution of 2.3 Å and 1.7 Å, respectively (see below), and compared with the respective structures of the wild-type enzyme (PDB codes 1KFK E(Ain) and 1KFJ E(Aex₁)). The complex obtained in the presence of L-Ser was produced by soaking the preformed crystals of βQ114N for 10 min in a solution containing a high concentration of L-Ser, just as described for other wild-type and mutant E(Aex₁) complexes (6). Although the resulting mutant structures display secondary and tertiary structures similar to those observed in other tryptophan synthase complexes (1, 5, 6, 9, 35), there are distinct differences at the active site of the β-subunit. In the case of the $^{\beta Q114N}$E(Ain) structure, weak electron density was observed for the side chain of βK87 to which the cofactor is usually covalently bound in the internal aldimine state. Moreover, the density for the cofactor was not very well defined, indicating that the electron density reflects either a mobile compound or several different structural states. Given that the spectroscopic results

show two distinct absorption bands instead of one (see paragraph above, Figure 4), it is likely that there is a mixture of states consisting of the covalently linked E(Ain) and a noncovalently bound, external aldimine-like species (data not shown). In the crystals soaked for 10 min with L-Ser, the cofactor molecule at the β-site appears to be fully occupied, showing electron density of an α-aminoacrylate-like compound (see next paragraph). Close inspection, however, revealed that the β-subunit still displays features of at least two different structural states, the open and the closed conformations of the β-domain. This is in line with the solution kinetic studies (see Figure 5A) which have established that the 10 min incubation period with L-Ser used for soaking yields the 320 nm species and is insufficient to allow completion of the conversion to the 506 nm species which displays a closed β-subunit (see below). Because refinement of the mixture of different structural states with varying occupancies for the E(Ain) and the E(Aex₁) complexes of the βQ114N mutant was unsuccessful, these structures are not described further and have not been deposited with the PDB.

The Overall Structure of the βQ114N (L-Ser, long soak) Complex. As described above, the $^{\beta Q114N}$E(Ain) short soak and $^{\beta Q114N}$E(Aex₁) structures were not structurally interpretable because of the mixture of states; thus, a second mutant E(Aex₁) complex was obtained. Since the spectral studies established that incubation overnight gives complete conversion of the mutant to the 506 nm species (Figures 5A and C), an extended L-Ser incubation time of about 24 h was used. In agreement with these findings, only those crystals that were soaked with L-Ser overnight (long soak) yielded a fully occupied complex that displays no residual density of additional intermediates or precursors.

The interdomain communication network found in the wild-type enzyme stabilizes and "primes" the α-active site in the absence of an ASL (9, 39). The α-subunit of the βQ114N complex obtained under the long soak conditions has an open conformation that is influenced by the closed conformation of the β-subdomain (see below). In the mutant E(Ain) structure, αL6 and the catalytic residues including, αD60 and αE49, are not visible; however, unexpectedly, all other secondary structure elements involved in ligand binding (e.g., residues αG212−αI214 (αL7) and αG234−αA236 (αH8′) that normally participate in the coordination of the phosphoryl group and hydrophobic groups) are well defined and closely match the conformations of the α-domains of the wild-type E(Aex₁) and E(Ain) structures (PDB codes 1KFJ and 1KFK). The superimposed structures give an average rmsd value of 0.4 Å. Additionally, despite large positional changes in the β-subunit resulting from β-closure, the structure of the interdomain interface between αL2 (αP53−αD60) and βH6 (βT165−βY181) is highly conserved. Due to the COMM domain movement that gives the closed β-domain structure, there is a shift of αL2 and associated regions (αS55-αP78, regions both preceding and succeeding the loop as well as sections connected by intramolecular interactions). Superposition of the mutant and wild-type E(Ain) (PDB code 1KFK) structures (Figures 9A and C) gives an average rmsd value of 0.9 Å. The superposition of the domains also reveals a second but smaller interface at the C-terminus consisting of part of βH6 and a loop (αC154−αD159) between αS5 and αH5. These
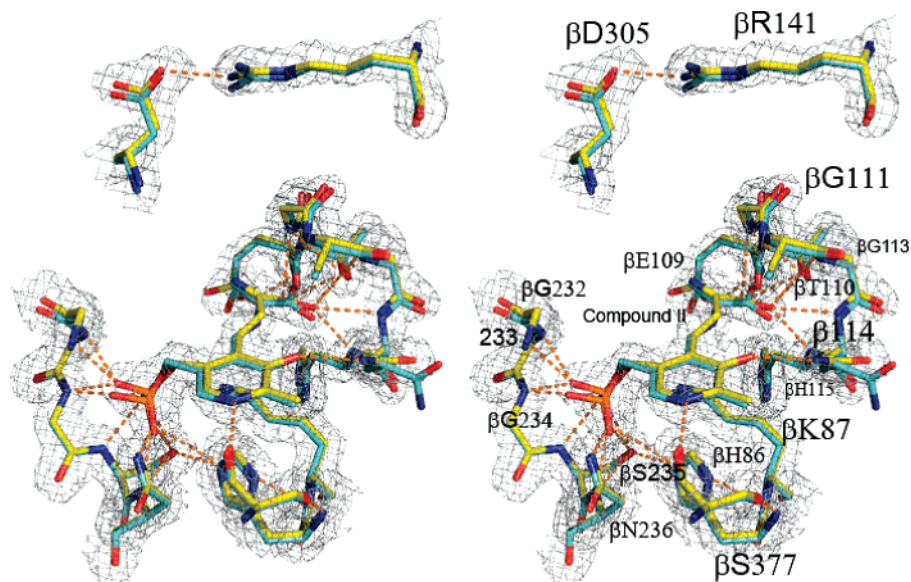
FIGURE 8: Stereoview of the structural model of compound II bound to the β-site with the final $2F_{obs} - F_{calc}$ electron density map contoured at 1σ. For comparison, the mutant complex structure, depicted in yellow, is superimposed with the (GP)E(A-A) complex (PDB code 2J9X), shown in cyan. Residues discussed in the text are labeled, orange dashed lines represent H-bonds in the $^{\beta Q114N}$E(compound II) complex.

auxiliary contacts between the side chain of αN157 and the hydroxyl group of βY181 and the main chain carbonyl of βI20 seem to act as a secondary contact point that is established when the β-domain closes.

The β-subunit of the complex obtained under the long soak conditions exhibits a closed conformation which has only been observed before for the βK87T E(Aex$_1$) and E(Aex$_2$) mutant structures generated by cocrystallization in the presence of either L-Ser or L-Trp and an α-site ligand (5), and recently in the closed (GP)E(A-A) complex of tryptophan synthase in the presence of Cs$^+$ at pH 6.5 (9) (viz., Figure 1). A comparison of these structures shows that all β-subunits with closed conformations closely resemble each other with rmsd values of 0.2 Å (PDB code 2J9X, Cs, low pH), 0.3 Å (PDB code 2TSY), respectively (Figure 9B).

The βQ114N Mutant β-Site Structure Reveals an Aminoacrylate-Like Compound. The β-site of the mutant complex displays some interesting features. The replacement of Gln with Asn at position 114 within βL3 leads to a shortening of the site chain by one methylene group ($\sim$1.5 Å). As a consequence of this change, βN114 in the mutant is rotated relative to βQ114 in the wild-type structure by 84° around Cβ toward the pyridine ring of the PLP cofactor, making an additional H-Bond (2.6 Å) between ND2 of βN114 and the phenolic hydroxyl group of the ring (Figure 8).

Clear electron density was observed for the cofactor itself after the first cycle of simulated annealing refinement, displaying an α-aminoacrylate-like electron density that was present in all βQ114N mutant complexes even in the absence of L-Ser. Both spectroscopic and structural evidence hint toward a different albeit similar molecule that is covalently bound to the cofactor. Together with the solution studies (Figures 4 and 5), the quantum chemical calculations (Table 4), and the positive identification of compound III by NMR as the species released by NaOH (see paragraph above, Figure 7), the electron density strongly supports the assignment of this molecule to the 506 nm species, named compound II (Scheme 3, Table 4).

Comparison of the β-sites of the mutant structure and the closed (GP)E(A-A) complex (9) reveals that compound II adopts a conformation in the active site that is similar to the α-aminoacrylate conformation (Figure 8). The carboxylate of compound II makes H-bonds to the γ-OH of βT110 and the backbone NH groups of βG111, βN114, and βH115. Additional contacts involve the region consisting of βG232$-$ βN236, βT190, and βH86 that coordinate the phosphoryl group and residue βS377 which aligns the pyridine ring. The H-bond linking the βD305 carboxylate to the γ-hydroxyl of βS292 and the H-bonded salt bridge between βD305 and βR141 are characteristic of the closed β-subunit conformation. These structural results indicate that the mutation shifts the relative thermodynamic stabilities of the open and closed conformations of the β-subunit in favor of the closed state.

DISCUSSION

Structure$-$Function Relationships at the α-Carboxylate Subsite in the β-Subunit of Tryptophan Synthase. βT110 and βQ114 are highly conserved residues located in loop βL3 of the domain that mediates communication between the α- and β-sites, the COMM domain (see Figure 1). These residues are also components of the α-carboxylate subsite and are involved in H-bonds with the intermediates that form with PLP during the β-reaction. These H-bonding interactions include the βQ114 main chain NH and the side chain hydroxyl group of βT110. Replacement of Gln by Asn at β114 *a priori* would seem to bring about a minor perturbation of the site resulting from a shortening of the side chain of the residue by only $\sim$1.5 Å at a location not directly involved with the substrate α-carboxylate. In contrast, replacing βT110 by Val removes a potentially important electrostatic interaction within βL3 that could impact the structural integrity of the loop that contacts the carboxyl group binding site. As documented in this report, both mutations cause profound changes in the catalytic and allosteric properties of tryptophan synthase.
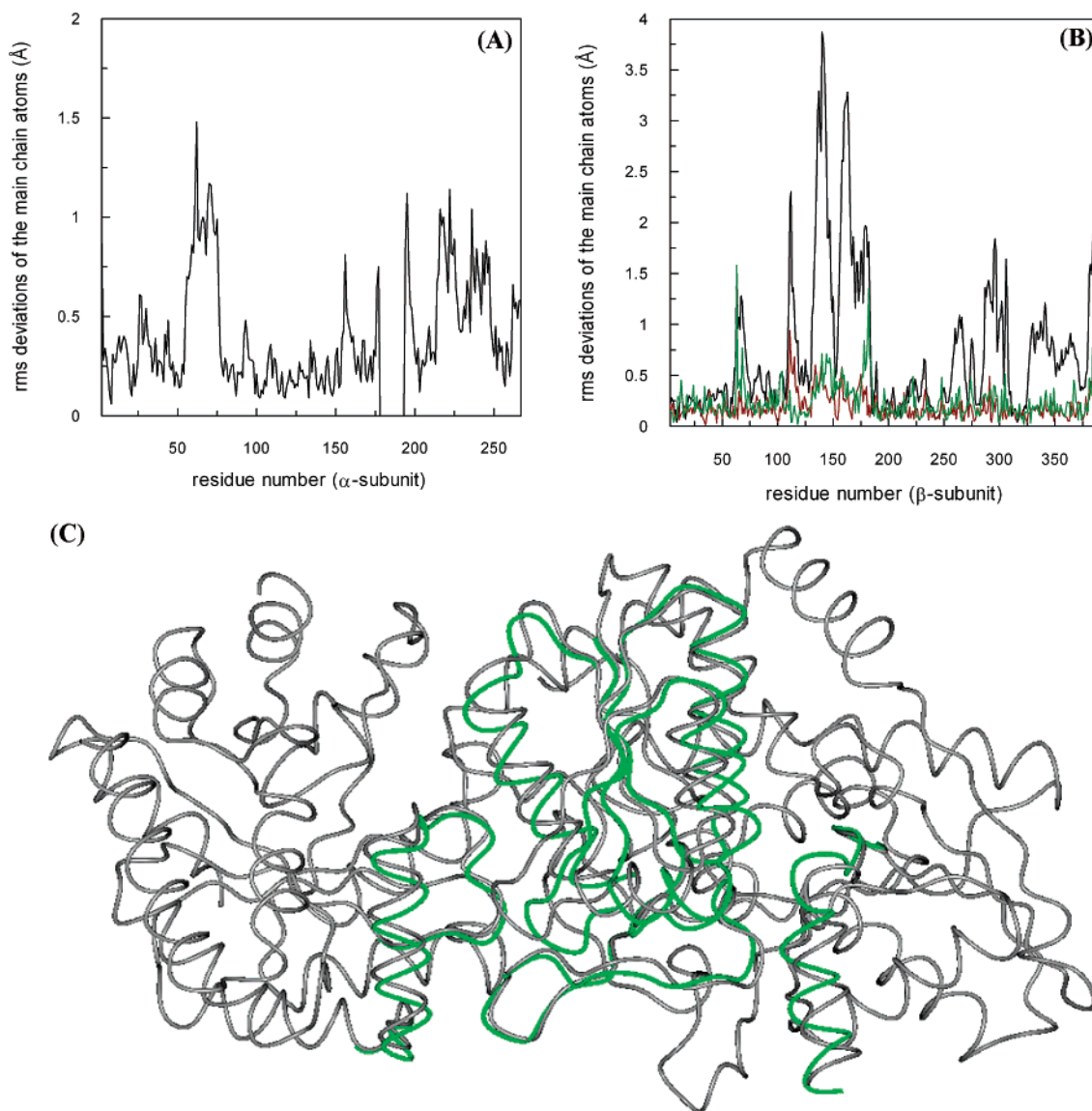
FIGURE 9: Structural comparison between the $^{\beta Q114N}$E(compound II) and the wt E(Ain) state. Plots show the rms deviation between the main chain atoms of the corresponding residues of the ASL-free E(Ain) state (PDB code 1KFK) and the mutant complex and other states (external aldimine and α-aminoacrylate) in stage I of the β-reaction [in (A) the α-subunit and in (B) the β-subunit]. The plots were generated by lsqkab. Black: $^{\beta Q114N}$E(compound II); red: E(Aex$_1$), PDB code 1KFJ; green: E(A-A), PDB code 1A5S. (C) Structural superposition of the wt E(Ain) structure (PDB code 1KFK, gray) and the $^{\beta Q114N}$E(compound II) complex in worm representation. For clarity, only those regions that were found to change significantly are displayed (green).

Origins of the Blue-Shifted Spectral Bands of the βT110V Mutant Assigned to the E(Ain) and E(Aex$_1$) Species. The evidence presented in Figure 2 and Table 2 indicates that the replacement of the polar hydroxyl of βT110 by a nonpolar methyl group alters the local microenvironment and interferes with the delicate balance of those electrostatic forces at the α-carboxylate subsite evolved to stabilize binding of the carboxylate moieties of substrate, intermediates, and product. Consequently, the blue-shifting of the long wavelength spectral bands assigned to E(Ain) and E(Aex$_1$) are consistent with a perturbed α-carboxylate binding site exhibiting decreased polarity.

Origins of the Impaired Catalytic Activity of the βT110V Mutant. The inability of the βT110V mutant to give significant amounts of the α-aminoacrylate intermediate (Figure 2) correlates with the greatly reduced activity of the mutant in the β- and αβ-reactions (Table 2). The allosteric effects due to the binding of Cs$^+$ to the β-subunit and to the

binding of ASLs to the α-subunit, respectively, have been found to be effective in rescuing other β-subunit mutants with impaired catalytic activity (*33, 34, 58, 65, 68−70*). However, the binding of a high affinity ASL (F9) (*39*) and the substitution of Cs$^+$ for Na$^+$ failed to rescue the βT110V mutant, presumably because the binding interactions with F9 and/or Cs$^+$ are insufficient to overcome the effects of mutation that distort the allosteric interface, as observed in the structure (Figure 3). The Thr to Val mutation leads to a change of those parts of the COMM domain that are crucial for the structural signaling of both domains. The widening of the β-active site by the shift of loop βL3 likely causes the decreased affinity of L-Ser. The rate of the β-reaction of the mutant enzyme is strongly reduced, and the mutant is not capable of producing pyruvate. Therefore, it can be concluded that impairment of E(A-A) formation is due either to the prevention of, or an unfavorable equilibrium for, formation of the external aldimine. Either explanation is in

line with the lack of electron density for the L-Ser moiety in the mutant structures.

Additional catalytic defects arise in the βT110V mutant from alterations in the communication interface between αL2 and βH6, leading to an uncoupling of the α- and β-reactions through the loss of allosteric communication in the enzyme. Although the α-subunit exhibits catalytic activity, no ligand could be observed in the structures obtained after incubation with α-site ligands that exhibit high affinity for the wild-type enzyme. The structure of the α-domain is very similar to the unligated α-domain of the wild-type protein (PDB code 1KFK). This observation suggests that the altered $\alpha-\beta$-subunit interface stabilizes the α-domain in the open (low activity) conformation characteristic of the wild-type internal aldimine, and this stabilization of the inactive conformation gives a mutant enzyme that no longer responds to the ligand upon binding, leading only to transient binding, reduced affinity, or a bound ASL that is too mobile to be observed in the crystal structure. Since ANS (8-anilino-1-naphthalenesulfonate) displacement (71) could not be employed to measure the actual affinity of the ligand for the enzyme because of the absence of allosteric communication between the sites in the mutant (the effect that ANS actually measures), neither of these possibilities could be excluded.

Altered Properies of the Catalytically Active βQ114N Mutant. While the fraction of βQ114N mutant that is not in the form of the 506 nm species exhibits catalytic activities in the α-, β-, and $\alpha\beta$-reactions that are very similar to the wild-type enzyme (Table 3), the UV/vis absorption spectra of the PLP intermediates are slightly perturbed by the mutation. The internal aldimine form of the active mutant exhibits a λ_{max} of 414 nm. Reaction with L-Ser (Scheme 3, Figure 5) gives a transient ~424 nm species that appears to be the L-Ser external aldimine together with the α-aminoacrylate external aldimine. This mixture undergoes further reaction to give a ~320 nm species (compound I, Scheme 3, Figures 5 and 8) which slowly converts to the 506 nm species (compound II). When reacted in the presence of the indole analogues/nucleophiles that are capable of reacting with E(A-A), the resulting quinonoid species exhibit spectra that are significantly red-shifted (~10 nm) in comparison to the wild-type enzyme (Figure 6). These perturbed spectra demonstrate that the mutation causes conformational changes in the β-subunit and affects the microenvironments of these chromophores.

Origins of the 506 nm Absorption Band in the βQ114N Mutant. The experiments presented in Figures 4−7 and Table 3 established the following: (a) The fraction of βQ114N mutant that is not in the form of the 506 nm species exhibits nearly normal activities in the α-, β-, and $\alpha\beta$-reactions (Table 3). (b) In stage I of the β-reaction, the α-aminoacrylate intermediate ($\lambda_{max} \sim 320$ nm) formed with the mutant follows a side path wherein this intermediate is cleaved giving α-aminoacrylate and the internal aldimine (Scheme 3, Figures 4 and 5). The α-aminoacrylate formed is a reactive species that partitions between reaction with water to give pyruvate (a well-known side-reaction of tryptophan synthase) and nucleophilic attack on E(Ain) to form a C−C bond at C-4′ of the PLP moiety of the internal aldimine, inactivating the tightly bound cofactor. For every ~50 turnovers of the α-aminoacrylate external aldimine to α-aminoacrylate, ~49 α-aminoacrylate molecules are converted to pyruvate, and

one inactivates a β-site via reaction with the internal aldimine. The resulting inactivated, enzyme-bound species undergoes further reaction over ~24 h, giving a conjugated species with $\lambda_{max} = 506$ nm, proposed to be compound II (Scheme 3). (c) Treatment of the 506 nm species with NaOH releases the covalently modified coenzyme, giving a 426 nm species identical (via UV/vis and ^{1}H NMR) to the species obtained with other tryptophan synthase mutants (33, 34), designated compound III. These assignments of compounds II and III are supported by the good agreement of the experimentally measured and quantum chemically calculated absorption maxima (Table 4).

Structural Consequences of the Gln → Asn Substitution at Position 114 of the β-Subunit. It has long been known that the reaction of L-Ser triggers an allosteric conformational change that enhances catalytic cleavage in the α-subunit (2−4, 6, 12, 40, 64, 72). Brzovic et al. (2) established that this activation is due to formation of the α-aminoacrylate intermediate at the β-site. It has been proposed that when E(Aex$_1$) is converted to E(A-A) in the $\alpha\beta$-reaction cycle, both subdomains have been switched to the closed conformations and the α- and β-sites are both activated (2, 4, 8, 73).

The βQ114N mutant reported here displays some unique features not observed before. The structure of the mutant complex shows the α-subunit in its open conformation with an unoccupied active site. The β-subunit, however, shares all of the structural features of a closed α-aminoacrylate species (9) (Figures 8 and 9). This finding was surprising since it has proven difficult to produce crystals of the closed α-aminoacrylate complex of tryptophan synthase under the conditions normally used for data collection (temperature 100 K, pH 7.8, Na$^+$) because of a temperature-dependent equilibrium between the E(Aex$_1$) and E(A-A) states, favoring the former, which is affected further by pH, ASLs, and monovalent cations (MVCs) (9, 45, 46, 58, 67, 70). Nevertheless, kinetic evidence predicts an E(A-A) state with a closed β-domain in solution (2, 8, 31, 45, 46, 63, 64, 66, 73, 74), and a closed crystal structure of the Cs$^+$ form of the (GP)E(A-A) complex at pH 6.5 has been determined recently (9) (see Figure 1). During the catalytic cycle, it is necessary for both the α- and β-sites to switch between open and closed states to prevent indole from escaping when IGP is cleaved in the α-reaction (2, 4, 9, 39, 60, 73). Interestingly and despite closure of the β-subunit in the βQ114N mutant after reaction with L-Ser, the α-subunit is not in the closed conformation. This finding clearly demonstrates that the β-subunit has not induced closure of the α-subunit on it own, and that closure of the α-subunit occurs when an α-site ligand is bound.

Implications of the βQ114N Mutation for Structure−Function Relationships in PLP Enzyme Reaction Specificity. While Dunathan's hypothesis (Scheme 2) provides a mechanistic framework for explaining how different PLP enzymes select for a particular reaction specificity (e.g., decarboxylation vs transamination or β-replacement) (16, 17, 20−23, 28), the hypothesis does not readily explain why in the tryptophan synthase system the transiminations of the substrate and product external aldimine species are facile, while transimination of the α-aminoacrylate external aldimine is rendered unfavorable (Scheme 4). Since α-aminoacrylate is a reactive nucleophile (an enamine), it is reasonable to

Scheme 4: Interconversion of the L-Ser, α-Aminoacrylate, and L-Trp External Aldimine Species
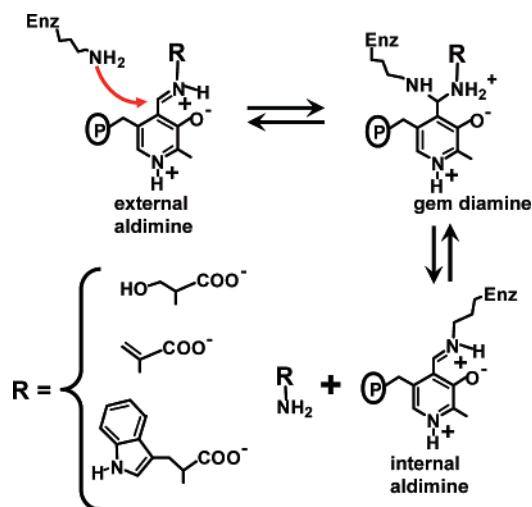
expect that the site structure has evolved to select against its release during catalysis, thus preventing its reactions with the internal aldimine electrophile.

The conversion of the α-aminoacrylate external aldimine to internal aldimine and α-aminoacrylate requires no more chemical catalysis to occur than does either the conversion of the L-Trp external aldimine to the internal aldimine with release of L-Trp, or the conversion of the L-Ser external aldimine back to L-Ser with formation of the internal aldimine (Scheme 4). From a chemical perspective, the α-aminoacrylate external aldimine should be slightly more reactive than either the L-Ser or L-Trp external aldimines. In each of these transimination reactions (Scheme 4), the ε-amino group of βK87 initiates a nucleophilic attack on the external aldimine species at the C-4′ carbon to give the corresponding *gem*-diamine species, which then collapses to the internal aldimine with release of the amino acid (α-aminoacrylate, L-Trp, or L-Ser). Like other PLP-requiring enzymes, tryptophan synthase has evolved to make the transimination processes facile for substrate and product external aldimines (processes along the catalytic path) but not for the α-aminoacrylate external aldimine (a side-reaction). This is also true for other PLP-requiring enzymes that involve reactive α-aminoacrylate internal aldimines in β-elimination and β-replacement reactions (*27, 28, 75−80*).

Since the transimination chemistry is essentially the same for the L-Ser, L-Trp, and α-aminoacrylate species, side chain structure only matters within the context of catalytic site conformation. Therefore, the explanation for facile conversions of the L-Ser and L-Trp external aldimines and retardation of the α-aminoacrylate external aldimine reaction in the wild-type enzyme must be conformational (steric) not chemical.[2] Since both the wild-type and mutant enzymes exhibit similar activities in the physiological reactions and in pyruvate formation (Table 3), both must "catalyze" the transimination reaction of the α-aminoacrylate external aldimine to about the same extent. The difference is that the wild-type enzyme efficiently releases α-aminoacrylate, thereby avoiding adduct formation with the internal aldimine. In contrast, the mutant has a significant rate of adduct formation with α-aminoacrylate.

A priori, the enamine reaction of α-aminoacrylate with the coenzyme could be facilitated by electrostatic/base catalysis. Adduct formation occurs at a rate that is ∼1/50th of the rate of pyruvate formation via partitioning of α-aminoacrylate between reaction with water (presumably a nonenzymatic process) and reaction with the coenzyme. For example, a side chain carboxylate within the site could facilitate the nucleophilic attack of α-aminoacrylate on the internal aldimine by stabilizing the development of positive charge on the enamine N as the C−C bond is formed between the C-3 of α-aminoacrylate and the C-4′ of the internal aldimine. However, inspection of the X-ray structure of the adduct shows no carboxylate (or similar group) near enough to be effective in this role: the nearest carboxylates, βE109 and βD305, are respectively 8.2 Å and 9.9 Å distant. Furthermore the βD305 carboxylate is tied up in the H-bonded salt bridge with βR141, and this salt bridge is critically important for stabilizing the closed conformation of the β-subunit. Alternatively, the ε-NH₂ group of βLys87 is ∼4.5 Å distant from the enamine N and appears to be too far to provide base assistance to the attack unless there is movement of the ε-NH₂ group. Thus, there is no clear candidate within the site to facilitate the attack.

Therefore, the most likely explanation for the different fates of α-aminoacrylate is that the mutation either orients or immobilizes the PLP via the H-bond between βN114 and the phenolic oxygen atom of the PLP ring for attack by the α-aminoacrylate, or that the mutation stabilizes the closed conformation, sequestering α-aminoacrylate within the site, thereby increasing the probability of reaction with the coenzyme. Because the release of α-aminoacrylate (presumably via a switch to the open conformation) is rapid in the wild-type enzyme compared to the rate of adduct formation, attack of α-aminoacrylate on the wild-type internal aldimine is not significant. This conclusion suggests that the mutation introduces a defect in the mechanism for switching the β-site between open and closed conformations.[3]

ACKNOWLEDGMENT

REFERENCES

1. Schneider, T. R., Gerhardt, E., Lee, M., Liang, P. H., Anderson, K. S., and Schlichting, I. (1998) Loop closure and intersubunit communication in tryptophan synthase, *Biochemistry 37*, 5394−5406.
2. Brzovic, P. S., Ngo, K., and Dunn, M. F. (1992) Allosteric interactions coordinate catalytic activity between successive

---

[2] This is true even if the difference in reactivities is the consequence of a difference in protonation states (for example, protonation of the βK87 ε-amino group or deprotonation of the external aldimine nitrogen of the α-aminoacrylate external aldimine) because maintenance of different protonation states would require different conformation states.

---

[3] In this regard, Brzovic et al. (*2*) demonstrated that the L-Ser and L-Trp external aldimines and the *gem*-diamine species do not activate the α-site, implying that these species favor the low activity state of the β-site (see refs *1, 3−6*). In contrast to this behavior, the α-aminoacrylate external aldimine and quinonoid species strongly activate the α-site, confirming that these species give a different β-site conformation: the conformation that triggers the cascade of allosteric signaling that mediates α-site activation (*2−4, 7, 8*). The accumulated evidence indicates this β-site state has a closed conformation (*9*).

metabolic enzymes in the tryptophan synthase bienzyme complex, *Biochemistry 31*, 3831−3839.

3. Leja, C. A., Woehl, E. U., and Dunn, M. F. (1995) Allosteric linkages between β-site covalent transformations and α-site activation and deactivation in the tryptophan synthase bienzyme complex, *Biochemistry 34*, 6552−6561.

4. Pan, P., Woehl, E., and Dunn, M. F. (1997) Protein architecture, dynamics and allostery in tryptophan synthase channeling, *Trends Biochem. Sci. 22*, 22−27.

5. Rhee, S., Parris, K. D., Hyde, C. C., Ahmed, S. A., Miles, E. W., and Davies, D. R. (1997) Crystal structures of a mutant (βK87T) tryptophan synthase α2β2 complex with ligands bound to the active sites of the α- and β-subunits reveal ligand-induced conformational changes, *Biochemistry 36*, 7664−7680.

6. Kulik, V., Weyand, M., Seidel, R., Niks, D., Arac, D., Dunn, M. F., and Schlichting, I. (2002) On the role of alphaThr183 in the allosteric regulation and catalytic mechanism of tryptophan synthase, *J. Mol. Biol. 324*, 677−690.

7. Miles, E. W., Rhee, S., and Davies, D. R. (1999) The molecular basis of substrate channeling, *J. Biol. Chem. 274*, 12193−12196.

8. Harris, R. M., Ngo, H., and Dunn, M. F. (2005) Synergistic effects on escape of a ligand from the closed tryptophan synthase bienzyme complex, *Biochemistry 44*, 16886−16895.

9. Ngo, H., Kimmich, N., Harris, R., Niks, D., Blumenstein, L., Kulik, V., Barends, T. R., Schlichting, I., and Dunn, M. F. (2007) Allosteric regulation of substrate channeling in tryptophan synthase: modulation of the L-serine reaction in stage I of the β-reaction by α-site ligands, *Biochemistry 46*, 7740−7753.

10. Miles, E. W. (1979) Tryptophan synthase: structure, function, and subunit interaction, *Adv. Enzymol. Relat. Areas Mol. Biol. 49*, 127−186.

11. Metzler, D. E. (2001) *Biochemistry*, 2nd ed., pp 737−753, Academic Press, New York.

12. Yanofsky, C. and Crawford, I. P. (1972) Tryptophan Synthase, in *The Enzymes* (Boyer, P. D., Ed.) 7th ed., pp 1−31, Academic Press, New York.

13. Miles, E. W. (1991) Structural basis for catalysis by tryptophan synthase, *Adv. Enzymol. Relat Areas Mol. Biol. 64*, 93−172.

14. Miles, E. W. (1995) *Subcellular Biochemistry*, pp 204−254, Plenum Press, New York.

15. Mehta, P. K., and Christen, P. (2000) The molecular evolution of pyridoxal-5′-phosphate-dependent enzymes, *Adv. Enzymol. Relat. Areas Mol. Biol. 74*, 129−184.

16. Dunathan, H. C. (1971) Stereochemical aspects of pyridoxal phosphate catalysis, *Adv. Enzymol. Relat. Areas Mol. Biol. 35*, 79−134.

17. Dunathan, H. C., and Voet, J. G. (1974) Stereochemical evidence for the evolution of pyridoxal-phosphate enzymes of various function from a common ancestor, *Proc. Natl. Acad. Sci. U.S.A 71*, 3888−3891.

18. Cronin, C. N., and Kirsch, J. F. (1988) Role of arginine-292 in the substrate specificity of aspartate aminotransferase as examined by site-directed mutagenesis, *Biochemistry 27*, 4572−4579.

19. Almo, S. C., Smith, D. L., Danishefsky, A. T., and Ringe, D. (1994) The structural basis for the altered substrate specificity of the R292D active site mutant of aspartate aminotransferase from E. coli, *Protein Eng. 7*, 405−412.

20. Fogle, E. J., Liu, W., Woon, S. T., Keller, J. W., and Toney, M. D. (2005) Role of Q52 in catalysis of decarboxylation and transamination in dialkylglycine decarboxylase, *Biochemistry 44*, 16392−16404.

21. Toney, M. D. (2005) Reaction specificity in pyridoxal phosphate enzymes, *Arch. Biochem. Biophys. 433*, 279−287.

22. Liu, W., Rogers, C. J., Fisher, A. J., and Toney, M. D. (2002) Aminophosphonate inhibitors of dialkylglycine decarboxylase: structural basis for slow binding inhibition, *Biochemistry 41*, 12320−12328.

23. Zhou, X., Jin, X., Medhekar, R., Chen, X., Dieckmann, T., and Toney, M. D. (2001) Rapid kinetic and isotopic studies on dialkylglycine decarboxylase, *Biochemistry 40*, 1367−1377.

24. Sun, S., and Toney, M. D. (1999) Evidence for a two-base mechanism involving tyrosine-265 from arginine-219 mutants of alanine racemase, *Biochemistry 38*, 4058−4065.

25. Inoue, Y., Kuramitsu, S., Inoue, K., Kagamiyama, H., Hiromi, K., Tanase, S., and Morino, Y. (1989) Substitution of a lysyl residue for arginine 386 of Escherichia coli aspartate aminotransferase, *J. Biol. Chem. 264*, 9673−9681.

26. Danishefsky, A. T., Onnufer, J. J., Petsko, G. A., and Ringe, D. (1991) Activity and structure of the active-site mutants R386Y

27. Burkhard, P., Tai, C. H., Ristroph, C. M., Cook, P. F., and Jansonius, J. N. (1999) Ligand binding induces a large conformational change in O-acetylserine sulfhydrylase from Salmonella typhimurium, *J. Mol. Biol. 291*, 941−953.

28. Aitken, S. M., and Kirsch, J. F. (2004) Role of active-site residues Thr81, Ser82, Thr85, Gln157, and Tyr158 in yeast cystathionine β-synthase catalysis and reaction specificity, *Biochemistry 43*, 1963−1971.

29. Likos, J. J., Ueno, H., Feldhaus, R. W., and Metzler, D. E. (1982) A novel reaction of the coenzyme of glutamate decarboxylase with L-serine O-sulfate, *Biochemistry 21*, 4377−4386.

30. Ueno, H., Likos, J. J., and Metzler, D. E. (1982) Chemistry of the inactivation of cytosolic aspartate aminotransferase by serine O-sulfate, *Biochemistry 21*, 4387−4393.

31. Ahmed, S. A., Ruvinov, S. B., Kayastha, A. M., and Miles, E. W. (1991) Mechanism of mutual activation of the tryptophan synthase alpha and beta subunits. Analysis of the reaction specificity and substrate-induced inactivation of active site and tunnel mutants of the beta subunit, *J. Biol. Chem. 266*, 21548−21557.

32. Jhee, K. H., McPhie, P., Ro, H. S., and Miles, E. W. (1998) Tryptophan synthase mutations that alter cofactor chemistry lead to mechanism-based inactivation, *Biochemistry 37*, 14591−14604.

33. Ferrari, D., Yang, L. H., Miles, E. W., and Dunn, M. F. (2001) Beta D305A mutant of tryptophan synthase shows strongly perturbed allosteric regulation and substrate specificity, *Biochemistry 40*, 7421−7432.

34. Ferrari, D., Niks, D., Yang, L. H., Miles, E. W., and Dunn, M. F. (2003) Allosteric communication in the tryptophan synthase bienzyme complex: roles of the β-subunit aspartate 305-arginine 141 salt bridge, *Biochemistry 42*, 7807−7818.

35. Weyand, M., Schlichting, I., Marabotti, A., and Mozzarelli, A. (2002) Crystal structures of a new class of allosteric effectors complexed to tryptophan synthase, *J. Biol. Chem. 277*, 10647−10652.

36. Weyand, M., Schlichting, I., Herde, P., Marabotti, A., and Mozzarelli, A. (2002) Crystal structure of the beta Ser178−> Pro mutant of tryptophan synthase. A "knock-out" allosteric enzyme, *J. Biol. Chem. 277*, 10653−10660.

37. Weyand, M., and Schlichting, I. (2000) Structural basis for the impaired channeling and allosteric inter-subunit communication in the beta A169L/beta C170W mutant of tryptophan synthase, *J. Biol. Chem. 275*, 41058−41063.

38. Woehl, E. U., and Dunn, M. F. (1995) Monovalent metal ions play an essential role in catalysis and intersubunit communication in the tryptophan synthase bienzyme complex, *Biochemistry 34*, 9466−9476.

39. Ngo, H., Harris, R., Kimmich, N., Casino, P., Niks, D., Blumenstein, L., Barends, T. R., Kulik, V., Weyand, M., Schlichting, I., and Dunn, M. F. (2007) Synthesis and characterization of allosteric probes of substrate channeling in the tryptophan synthase bienzyme complex, *Biochemistry 46*, 7713−7727.

40. Kawasaki, H., Bauerle, R., Zon, G., Ahmed, S. A., and Miles, E. W. (1987) Site-specific mutagenesis of the alpha subunit of tryptophan synthase from Salmonella typhimurium. Changing arginine 179 to leucine alters the reciprocal transmission of substrate-induced conformational changes between the alpha and beta 2 subunits, *J. Biol. Chem. 262*, 10678−10683.

41. Ho, S. N., Hunt, H. D., Horton, R. M., Pullen, J. K., and Pease, L. R. (1989) Site-directed mutagenesis by overlap extension using the polymerase chain reaction, *Gene 77*, 51−59.

42. Miles, E. W., Bauerle, R., and Ahmed, S. A. (1987) Tryptophan synthase from Escherichia coli and Salmonella typhimurium, *Methods Enzymol. 142*, 398−414.

43. Yang, L., Ahmed, S. A., and Miles, E. W. (1996) PCR mutagenesis and overexpression of tryptophan synthase from Salmonella typhimurium: on the roles of beta2 subunit Lys-382, *Protein Expr. Purif. 8*, 126−136.

44. Peracchi, A., Mozzarelli, A., and Rossi, G. L. (1995) Monovalent cations affect dynamic and functional properties of the tryptophan synthase α 2 β 2 complex, *Biochemistry 34*, 9459−9465.

45. Woehl, E., and Dunn, M. F. (1999) Mechanisms of monovalent cation action in enzyme catalysis: the first stage of the tryptophan synthase β-reaction, *Biochemistry 38*, 7118−7130.

46. Woehl, E., and Dunn, M. F. (1999) Mechanisms of monovalent cation action in enzyme catalysis: the tryptophan synthase α-, β-, and α β-reactions, *Biochemistry 38*, 7131−7141.

47. Kabsch, W. (1993) Automatic Processing of Rotation Diffraction Data from Crystals of Initially Unknown Symmetry and Cell Constants, *J. Appl. Crystallogr. 26*, 795−800.

48. Brunger, A. T., Adams, P. D., Clore, G. M., DeLano, W. L., Gros, P., Grosse-Kunstleve, R. W., Jiang, J. S., Kuszewski, J., Nilges, M., Pannu, N. S., Read, R. J., Rice, L. M., Simonson, T., and Warren, G. L. (1998) Crystallography & NMR system: A new software suite for macromolecular structure determination, *Acta Crystallogr. D. Biol. Crystallogr. 54*, 905−921.

49. Jones, T. A., Zou, J. Y., Cowan, S. W., and Kjeldgaard, M. (1991) Improved methods for building protein models in electron density maps and the location of errors in these models, *Acta Crystallogr. A 47 (Pt 2)*, 110−119.

50. McRee, D. E. (1999) XtalView/Xfit—A versatile program for manipulating atomic coordinates and electron density, *J. Struct. Biol. 125*, 156−165.

51. Lee, C., Yang, W., and Parr, R. G. (1988) Development of the Colle-Salvetti correlation-energy formula into a functional of the electron density, *Phys. Rev. B: Condens. Matter Mater. 37*, 785−789.

52. Becke, A. D. (1993) Density-functional thermochemistry. III. The role of exact exchange, *J. Chem. Phys. 98*, 5648−5652.

53. Nakano, H. (1993) Quasi-Degenerate Perturbation-Theory with Multiconfigurational Self-Consistent-Field Reference Functions, *J. Chem. Phys. 99*, 7983−7992.

54. Nemukhin, A. V., Grigorenko, B. L., and Granovsky, A. A. (2004) Molecular modeling by using the PC GAMESS Program: From diatomic molecules to enzymes, *Moscow Univ. Chem. Bull. 45*, 75−102.

55. Schmidt, M. W., Baldridge, K. K., Boatz, J. A., Elbert, S. T., Gordon, M. S., Jensen, J. H., Koseki, S., Matsunaga, N., Nguyen, K. A., Su, S. J., Windus, T. L., Dupuis, M., and Montgomery, J. A. (1993) General Atomic and Molecular Electronic-Structure System, *J. Comput. Chem. 14*, 1347−1363.

56. Drewe, W. F., Jr., and Dunn, M. F. (1985) Detection and identification of intermediates in the reaction of L-serine with *Escherichia coli* tryptophan synthase via rapid-scanning ultraviolet-visible spectroscopy, *Biochemistry 24*, 3977−3987.

57. Drewe, W. F., Jr., and Dunn, M. F. (1986) Characterization of the reaction of L-serine and indole with *Escherichia coli* tryptophan synthase via rapid-scanning ultraviolet-visible spectroscopy, *Biochemistry 25*, 2494−2501.

58. Weber-Ban, E., Hur, O., Bagwell, C., Banik, U., Yang, L. H., Miles, E. W., and Dunn, M. F. (2001) Investigation of allosteric linkages in the regulation of tryptophan synthase: the roles of salt bridges and monovalent cations probed by site-directed mutation, optical spectroscopy, and kinetics, *Biochemistry 40*, 3497−3511.

59. Marabotti, A., De, B. D., Tramonti, A., Bettati, S., and Mozzarelli, A. (2001) Allosteric communication of tryptophan synthase. Functional and regulatory properties of the beta S178P mutant, *J. Biol. Chem. 276*, 17747−17753.

60. Casino, P., Niks, D., Ngo, H., Pan, P., Brzovic, P., Blumenstein, L., Barends, T. R., Schlichting, I., and Dunn, M. F. (2007) Allosteric regulation of tryptophan synthase channeling: the internal aldimine probed by *trans*-3-indole-3′-acrylate binding, *Biochemistry 46*, 7728−7739.

61. Metzler, C. M., Cahill, A. E., Petty, S., Metzler, D. E., and Lang, L. (1985) The widespread applicability of lognormal curves for the description of absorption-spectra, *Appl. Spectrosc. 39*, 333−339.

62. Roy, M., Keblawi, S., and Dunn, M. F. (1988) Stereoelectronic control of bond formation in Escherichia coli tryptophan synthase: substrate specificity and enzymatic synthesis of the novel amino acid dihydroisotryptophan, *Biochemistry 27*, 6698−6704.

63. Harris, R. M., and Dunn, M. F. (2002) Intermediate trapping via a conformational switch in the Na(+)-activated tryptophan synthase bienzyme complex, *Biochemistry 41*, 9982−9990.

64. Anderson, K. S., Miles, E. W., and Johnson, K. A. (1991) Serine modulates substrate channeling in tryptophan synthase. A novel intersubunit triggering mechanism, *J. Biol. Chem. 266*, 8020−8033.

65. Brzovic, P. S., Sawa, Y., Hyde, C. C., Miles, E. W., and Dunn, M. F. (1992) Evidence that mutations in a loop region of the alpha-subunit inhibit the transition from an open to a closed conformation in the tryptophan synthase bienzyme complex, *J. Biol. Chem. 267*, 13028−13038.

66. Hur, O., Niks, D., Casino, P., and Dunn, M. F. (2002) Proton transfers in the β-reaction catalyzed by tryptophan synthase, *Biochemistry 41*, 9991−10001.

67. Schiaretti, F., Bettati, S., Viappiani, C., and Mozzarelli, A. (2004) pH dependence of tryptophan synthase catalytic mechanism: I. The first stage, the beta-elimination reaction, *J. Biol. Chem. 279*, 29572−29582.

68. Brzovic, P. S., Hyde, C. C., Miles, E. W., and Dunn, M. F. (1993) Characterization of the functional role of a flexible loop in the α-subunit of tryptophan synthase from *Salmonella typhimurium* by rapid-scanning, stopped-flow spectroscopy and site-directed mutagenesis, *Biochemistry 32*, 10404−10413.

69. Rowlett, R., Yang, L. H., Ahmed, S. A., McPhie, P., Jhee, K. H., and Miles, E. W. (1998) Mutations in the contact region between the α and β subunits of tryptophan synthase alter subunit interaction and intersubunit communication, *Biochemistry 37*, 2961−2968.

70. Fan, Y. X., McPhie, P., and Miles, E. W. (2000) Regulation of tryptophan synthase by temperature, monovalent cations, and an allosteric ligand. Evidence from Arrhenius plots, absorption spectra, and primary kinetic isotope effects, *Biochemistry 39*, 4692−4703.

71. Pan, P., and Dunn, M. F. (1996) β-Site covalent reactions trigger transitions between open and closed conformations of the tryptophan synthase bienzyme complex, *Biochemistry 35*, 5002−5013.

72. Kirschner, K., Lane, A. N., and Strasser, A. W. (1991) Reciprocal communication between the lyase and synthase active sites of the tryptophan synthase bienzyme complex, *Biochemistry 30*, 472−478.

73. Dunn, M. F., Aguilar, V., Brzovic, P., Drewe, W. F., Jr., Houben, K. F., Leja, C. A., and Roy, M. (1990) The tryptophan synthase bienzyme complex transfers indole between the α- and β-sites via a 25−30 Å long tunnel, *Biochemistry 29*, 8598−8607.

74. Phillips, R. S., Miles, E. W., Holtermann, G., and Goody, R. S. (2005) Hydrostatic pressure affects the conformational equilibrium of *Salmonella typhimurium* tryptophan synthase, *Biochemistry 44*, 7921−7928.

75. Hwang, C. C., Woehl, E. U., Minter, D. E., Dunn, M. F., and Cook, P. F. (1996) Kinetic isotope effects as a probe of the β-elimination reaction catalyzed by *O*-acetylserine sulfhydrylase, *Biochemistry 35*, 6358−6365.

76. Tai, C. H., Yoon, M. Y., Kim, S. K., Rege, V. D., Nalabolu, S. R., Kredich, N. M., Schnackerz, K. D., and Cook, P. F. (1998) Cysteine 42 is important for maintaining an integral active site for *O*-acetylserine sulfhydrylase resulting in the stabilization of the α-aminoacrylate intermediate, *Biochemistry 37*, 10597−10604.

77. Phillips, R. S., Sundararaju, B., and Faleev, N. G. (2000) Proton transfer and carbon-carbon bond cleavage in the elimination of indole catalyzed by *Escherichia coli* tryptophan indole-lyase, *J. Am. Chem. Soc. 122*, 1008−1014.

78. Jhee, K. H., Niks, D., McPhie, P., Dunn, M. F., and Miles, E. W. (2001) The reaction of yeast cystathionine β-synthase is rate-limited by the conversion of aminoacrylate to cystathionine, *Biochemistry 40*, 10873−10880.

79. Jhee, K. H., Niks, D., McPhie, P., Dunn, M. F., and Miles, E. W. (2002) Yeast cystathionine β-synthase reacts with L-allothreonine, a non-natural substrate, and L-homocysteine to form a new amino acid, 3-methyl- L-cystathionine, *Biochemistry 41*, 1828−1835.

80. Phillips, R. S., Chen, H. Y., and Faleev, N. G. (2006) Aminoacrylate intermediates in the reaction of *Citrobacter freundii* tyrosine phenol-lyase, *Biochemistry 45*, 9575−9583.